UNSUPERVISED DETECTION OF OPIUM POPPY FIELDS IN AFGHANISTAN FROM EO-1 HYPERION DATA

JIANJUN WANG

September 2013

TECHNICAL REPORT
NO. 286

UNSUPERVISED DETECTION OF OPIUM POPPY FIELDS IN AFGHANISTAN FROM EO-1 HYPERION DATA

Jianjun Wang

Department of Geodesy and Geomatics Engineering
University of New Brunswick
P.O. Box 4400
Fredericton, N.B.
Canada
E3B 5A3

September 2013

© Jianjun Wang, 2013

PREFACE

This technical report is a reproduction of a thesis submitted in partial fulfillment of the requirements for the degree of Master of Science in Engineering in the Department of Geodesy and Geomatics Engineering, September 2013. The research was supervised by Dr. Yun Zhang, and funding was provided by the Canada Research Chair (CRC) Program.

As with any copyrighted material, permission to reprint or quote extensively from this report must be received from the author. The citation to this work should appear as follows:

Wang, Jianjun (2013). *Unsupervised Detection of Opium Poppy Fields in Afghanistan from E0-1 Hyperion Data*. M.Sc.E. thesis, Department of Geodesy and Geomatics Engineering, Technical Report No. 286, University of New Brunswick, Fredericton, New Brunswick, Canada, 102 pp.

ABSTRACT

Satellite remote sensing has special advantages for monitoring the extent of illegal drug production that causes serious problems to the global society. Although remote sensing has been used to monitor opium poppy fields, the main data employed were high-resolution images (≤ 1 m) like pan-sharpened IKONOS, QuickBird, etc. These images are costly, making the full coverage of the crop fields in a large area an expensive exercise. As an alternative, the imagery acquired by EO-1 Hyperion, the only available spaceborne hyperspectral sensor currently, is free. However, its spatial resolution is coarser (30 m). Until now, there is little evidence that poppy fields have been identified from aerial or satellite hyperspectral images. This thesis proposed two unsupervised methods (i.e., a MESMA-based one and a MTMF-based one), that could detect poppy fields in Afghanistan from Hyperion data directly. Comparing the two methods, the MTMF-based one has much higher computational efficiency. Moreover, the MTMF-based method performed well in both of the two main environments in Afghanistan. In addition, it was found that the moderate spatial resolution EO-1 Advanced Land Imager (ALI) multispectral data could not produce reasonable detection of poppy fields in Afghanistan.

ACKNOWLEDGEMENTS

I would primarily thank my supervisor Dr. Yun Zhang for his continuous support and providing me with the opportunity to conduct this research. Without the support, the research would not have been possible. In addition, I would like to thank Dr. Zhang for supervising and providing me with proper guidance to complete the research and this thesis.

I would like to express on my sincere gratitude to Dr. Coen Bussink of United Nations Office on Drugs and Crime for providing their groundtruth data of opium poppy fields in Afghanistan, as well as for his constructive comments

I would extend my thanks to the staff at GGE, especially David Fraser and Sylvia Whitaker. They helped me out with the software and the academic procedures at UNB.

I would also like to thank all the members in the research group of Dr. Zhang for their help and friendships.

Last but not least, I would like to thank my wife and my parents for their patience.

TABLE OF CONTENTS

ABSTRACT ii

ACKNOWLEDGEMENTS iii

List of Tables viii

List of Figures ix

List of Symbols and Abbreviations..... xi

CHAPTER 1. INTRODUCTION 1

1.1 Thesis Structure 2

1.2 Background of the Opium Poppy 3

1.3 Opium Poppy Field Detection in Remote Sensing 7

1.3.1 Studies Using Multispectral Data 7

1.3.2 Studies Using Hyperspectral Data 9

1.3.3 Research Problem 10

1.4 Research Objective 11

1.5 Proposed Methodology 12

1.6 Overview of Each Chapter 13

References 14

CHAPTER 2. REMOTE SENSING OF OPIUM POPPY FIELDS USING EO-1 HYPERION HYPERSPECTRAL DATA: AN EXAMPLE IN AFGHANISTAN 16

Abstract 16

2.1 Introduction 17

2.2 Study Area and Materials 20

2.2.1 Study Area 20

2.2.2 Materials 21

2.3 Methodology 21
2.3.1 Hyperion Hyperspectral Data Pre-processing 23
2.3.2 Endmember Determination 24
2.3.3 Poppy Fraction Value Determination 27
2.4 Results and Discussion 29
2.5 Conclusions 34
Acknowledgements 35
References 36
CHAPTER 3. AN UNSUPERVISED MTMF-BASED METHOD FOR DETECTING OPIUM POPPY FIELDS IN HELMAND, AFGHANISTAN, FROM EO-1 HYPERION DATA 39
Abstract 39
3.1 Introduction 40
3.1.1 Background 40
3.1.2 Previous Work 41
3.1.2.1 Work of Other Researchers 41
3.1.2.2 Work of Wang et al. (2013) 43
3.2 Study Area and Materials 44
3.2.1 Study Area 44
3.2.2 Materials 46
3.3 Methodology 46
3.3.1 Hyperion Data Pre-processing 46
3.3.2 Endmember Determination of Main Vegetation Components 48
3.3.3 Poppy Pixel Determination 50
3.3.4 Detection Accuracy Assessment 52

3.4. Results 52

3.4.1 Effects of Involving More Endmembers in Each Component 52

3.4.2 Effects of Using Different Infeasibility Thresholds 53

3.4.3 Effects of Using Various MF Thresholds 54

3.4.4 Poppy Distribution Map 56

3.5 Discussion and Conclusions 57

Acknowledgements 60

References 61

CHAPTER 4. AN UNSUPERVISED APPROACH TO DETECT OPIUM POPPY FIELDS IN BATI KOT, NANGARHAR, AFGHANISTAN, USING EO-1 HYPERION DATA 64

Abstract 64

4.1 Introduction 65

4.2 Study Area 67

4.3 Data and Methodology 68

4.3.1 Data 68

4.3.2 Methodology 69

4.4 Results 74

4.5 Discussion and Conclusions 75

Acknowledgements 76

References 77

CHAPTER 5. CAN EO-1 ALI DATA DETECT OPIUM POPPY FIELDS IN HELMAND, AFGHANISTAN? 78

Abstract 78

5.1 Introduction 79

5.2 Data and Methodology 82
5.2.1 Data 82
5.2.2 Methodology 82
5.2.2.1 ALI Multispectral Data Pre-processing 83
5.2.2.2 Endmember Determination 83
5.2.2.3 Poppy Pixels Determination 86
5.3 Results and Discussion 86
5.4 Conclusions 89
Acknowledgements 90
References 90
CHAPTER 6. CONCLUSIONS AND RECOMMENDATIONS.....94
6.1 Summary of the Research 94
6.2 Contributions of the Research 96
6.3 Recommendations for Further Research 98
References 99
APPENDIX-I ENDMEMBER 101
Curriculum Vitae

LIST OF TABLES

Table 2.1 Number of MESMA models used…….…… 29

Table 2.2 Comparison of detection accuracies of poppy pixels. The “em” refers to “endmember”. …… 30

Table 2.3. Comparison of detection accuracies of poppy pixels when threshold of RMSE difference (i.e., >0.05%) was used against when no RMSE was used. The MSEMA-based methodology with 2- and 3-endmember models was applied to detect poppy fields.…… ……..……. 32

Table 3.1 Comparison of poppy field detection accuracies when different PPI thresholds, the same MF threshold (MF>0) and the same infeasibility threshold (Infeasibility<6) were used. Here, “multiple” refers that multiple endmembers were used, while “average” refers that an averaged endmember was used… 52

Table 3.2 Comparison of poppy field detection accuracies when the same PPI threshold (PPI≥2000), the same MF threshold (MF>0) but different infeasibility thresholds were used.……54

LIST OF FIGURES

Figure 1.1 Thesis structure 3

Figure 1.2 Opium Poppy (Source: Otto Wilhelm Thome Flora von Deutschland, Osterreich und der Schweiz 1885, Gera, Germany) 5

Figure 1.3 Global potential production (a) and illicit cultivation (b) of opium poppy during 1997-2011 (source: World Drug Report 2012).....…… 6

Figure 2.1 Study area. ..... …… 20

Figure 2.2 Methodology workflow. 22

Figure 2.3 The 31 pure vegetation pixels formed two distinct vegetation clusters, Components A (bottom left) and B (top right) in the n-Dimensional Visualizer in ENVI. The numbers referred to MNF band numbers…..……26

Figure 2.4 Spectral profile of averaged reflectance of endmembers in the two vegetation clusters, i.e., Components A and B, respectively……. 27

Figure 2.5 Poppy distribution map (a) retrieved from an EO-1 Hyperion image over the study area acquired on March 11, 2009. Surrogate groundtruth map of poppy (c1, and its subset c2) only covering the area within the box “b1” was compared with counterpart (b1, and its subset b2). Black pixels referred to poppy fields.. 33

Figure 3.1 Study area. .....……..…..45

Figure 3.2 The pure vegetation pixels formed two distinct vegetation clusters in the n-Dimensional Visualizer in ENVI, no matter either 2000 (a) or 1500 (b) was used as a PPI threshold. The numbers in the subfigures referred to MNF band numbers……..... 49

Figure 3.3 Workflow of poppy pixel determination in the MTMF-based methodology. The same set of thresholds was used for poppy and wheat..... 51

Figure 3.4 Comparison of poppy field detection accuracies when the same PPI threshold (PPI≥2000), the same infeasibility threshold (Infeasibility<6) but different MF thresholds were used. The "multiple" refers that multiple endmembers were used, while "average" refers that an averaged endmember was used…55

Figure 3.5 Poppy distribution map (a) retrieved from an EO-1 Hyperion image over the study area acquired on March 11, 2009. Groundtruth map of poppy (c1, and its subset c2) only covered the area within the box “b1” was compared with counterpart (b1, and its subset b2)……..……..... 57

Figure 3.6 Probability accumulation percentage verse infeasibility score. 58

Figure 4.1 Study area of Bati Kot, Nangarhar, Afghanistan. 67

Figure 4.2 The 207 vegetation endmembers formed three distinct vegetation clusters, i.e., Components A (poppy), B (wheat) and C (tree) in the n-Dimensional Visualizer in the ENVI.. 71

Figure 4.3 Spectral profile of averaged reflectance of endmembers in the three vegetation clusters, i.e., Components A (poppy), B (wheat) and C (tree), respectively.. .....…… 72

Figure 4.4 Methodology workflow of poppy field determination. 73

Figure 4.5 Poppy field distribution comparison. (a) Poppy field distribution map of Nangarhar Province, Afghanistan, reproduced from "Afghanistan Opium Survey 2004" (UNODC, 2004). The red and green colors represented poppy fields and other vegetation fields, respectively. (b) Poppy field distribution map of the Bati Kot study area, enlarged from (a). (c) Poppy field distribution map of the Bati Kot study area retrieved from an EO-1 Hyperion image over the study area acquired on March 21, 2004. The black color represented poppy fields in (c)..... 74

Figure 5.1 Study area map. 81

Figure 5.2 The 30 pure vegetation pixels with NDVI $\geqslant$0.2 and with smaller reflectance at ALI Band 5 (red) than at Band 4 (green) formed two vegetation clusters, Components A (top left) and B (bottom right) in the n-Dimensional Visualizer in ENVI. Numbers 1-4 referred to MNF band numbers.....84

Figure 5.3 Spectral profile of averaged reflectance of endmembers in the two vegetation clusters, i.e., Components A (poppy) and B (wheat), respectively..... 85

Figure 5.4 Poppy distribution maps over the study area that were (a) retrieved from an EO-1 ALI image acquired on March 11, 2009, and (b) provided by UNODC……..... 87

LIST OF SYMBOLS AND ABBREVIATIONS

ALI Advanced Land Imager

ALOS Advanced Land Observing Satellite

ASTER Advanced Spaceborne Thermal Emission and Reflection Radiometer

DMC Disaster Monitoring Constellation

DN Digital Number

ENVI ENvironment for Visualizing Images

EO-1 Earth Observing-1

ETM+ Enhanced Thematic Mapper Plus

FLAASH Fast Line-of-sight Atmospheric Analysis of Spectral Hypercubes

GCP Ground Control Point

GPS Global Positioning System

ISODATA Self-Organizing Data Analysis Technique Algorithm

MESMA Multiple Endmember Spectral Mixture Analysis

MF Matched Filtering

MNF Minimum Noise Fraction

MRENDVI Modified Red Edge Normalized Difference Vegetation Index

MTMF Mixture Tuned Matched Filtering

NDVI Normalized Difference Vegetation Index

PPI Pixel Purity Index

RMSE Root Mean Square Error

ROI Regions of Interest

SMA Spectral Mixture Analysis

SPOT-5 Système Pour l'Observation de la Terre-5

sSMA Simple Spectral Mixture Analysis

SWIR Short Wave Infrared

TM Thematic Mapper

UNODC United Nations Office on Drugs and Crime

USGS United States Geological Survey

VNIR Visible-Near Infrared

CHAPTER 1

INTRODUCTION

This thesis aimed to find a practical and economical way to map poppy fields in Afghanistan under the strict constraints of the inaccessibility of field surveys and limited finances. The literature review found that a few researchers have explored the potential of using high resolution satellite multispectral images (≤ 1m), such as pan-sharpened IKONOS, to detect poppy fields. As these high resolution images are expensive, this thesis attempts to detect poppy fields from medium resolution EO-1 Hyperion hyperspectral data, free of charge, in Afghanistan through two proposed methods: an unsupervised Multiple Endmember Spectral Mixture Analysis (MESMA)-based method and an unsupervised Mixture Tuned Matched Filtering (MTMF)-based method respectively. Neither required training samples in detection. They produced similar detection accuracies, but the MTMF-based method worked much faster because it needs less computational power. It was found that the MTMF-based method also performed well in another study area with different environment in mountainous east Afghanistan. In addition, it was found that medium resolution multispectral imagery of EO-1 Advanced Land Imager (ALI) cannot detect poppy fields reliably.

This thesis is presented through the following papers:

Paper 1 (peer reviewed):

Wang, J.J., Y. Zhang, and C. Bussink (2013) "Remote Sensing of Opium Poppy Fields Using EO-1 Hyperion Hyperspectral Data: an Example in Afghanistan." *Proceedings of the 2013 Canadian Institute of Geomatics Annual Conference and the 2013*

International Conference on Earth Observation for Global Changes (EOGC'2013), 5-7 June 2013, Toronto, Ontario, Canada.

Its extended version "Unsupervised Multiple Endmember Spectral Mixture Analysis-based Detection of Opium Poppy Fields from An EO-1 Hyperion Image in Helmand, Afghanistan" has been submitted to *Science of the Total Environment*.

Paper 2 (peer reviewed):

Wang, J.J., Y. Zhang, and C. Bussink (2013) "An unsupervised MTMF-based method for detecting opium poppy fields in Helmand, Afghanistan, from EO-1 Hyperion data." (submitted to *International Journal of Remote Sensing*)

Paper 3 (peer reviewed):

Wang, J.J., and Y. Zhang (2013) "An unsupervised approach to detect opium poppy fields in Bati Kot, Nangarhar, Afghanistan, using EO-1 Hyperion data." (to be submitted to *Remote Sensing (peer-reviewed Open Access journal)*)

Paper 4 (peer reviewed):

Wang, J.J., Y. Zhang, and C. Bussink (2013) "Can EO-1 ALI data detect opium poppy fields in Helmand, Afghanistan?" (to be submitted to *Remote Sensing (peer-reviewed Open Access journal)*)

1.1 Thesis Structure

This paper-based thesis incorporates three journal papers and one published conference paper, together with chapters of "Introduction" and "Summary and Conclusions". The structure of the thesis is presented in Figure 1.1 below.

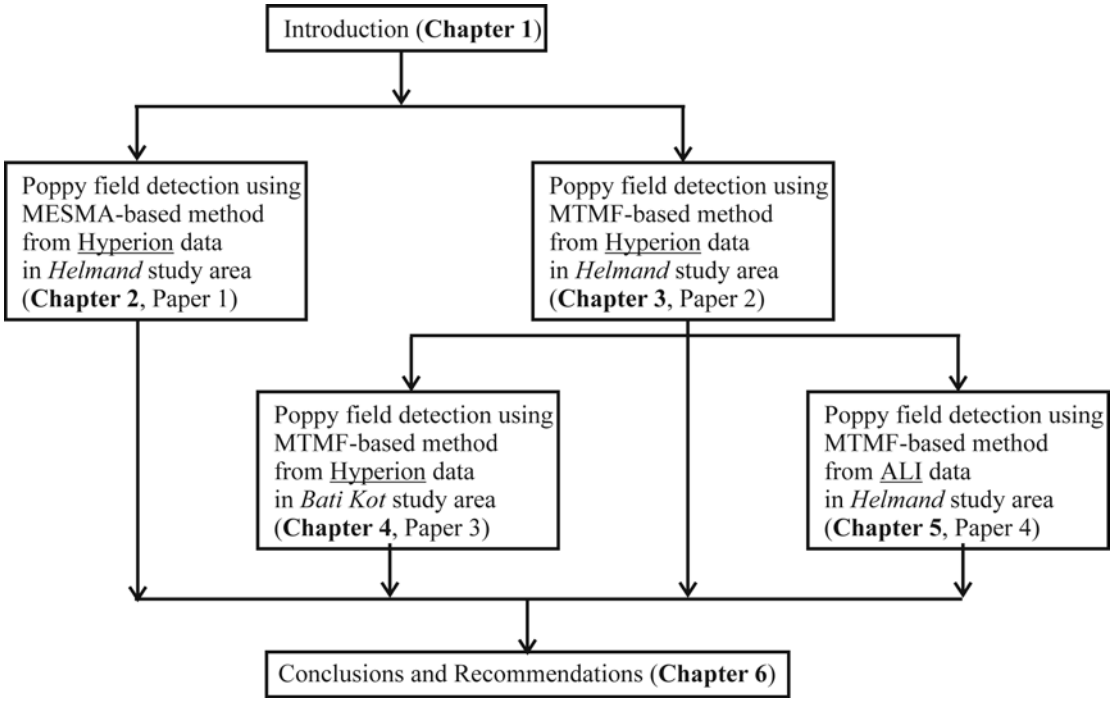

Figure 1.1 Thesis structure

1.2 Background of the Opium Poppy

Drug abuse is a serious problem worldwide. According to "World Drug Report 2012" (UNODC, 2012), of the world population between the ages of 15 and 64, about 1 in 20 people uses an illegal drug at least once a year; approximately 1 in 40 people uses drugs more regularly. Drug abuse undermines economic and social development and leads to crime, instability, insecurity and the spread of HIV. UNODC (2012) estimated that drug-related deaths accounted for 0.5-1.3% of all-cause mortality among those aged 15-64 in 2010 globally.

Opium is the source of many narcotics, including morphine (and its derivative heroin), thebaine, codeine, papaverine, and noscapine (Wikipedia, 2013). Opium is derived from Opium poppy (i.e., *Papaver somniferum*; see Figure 1.2). Sader (1991),

taking Afghanistan as an example, introduced the general characteristics of opium poppy cultivation. In Afghanistan, the main competing crops of poppy are wheat, corn, cotton and vegetables. The growers follow a double cropping pattern. Poppies are planted in the fall and harvested in the spring. Corn, cotton, or vegetables are planted in the spring or early summer and harvested in the fall. The next rotation would be wheat, fall or winter planted and harvested in early summer. Corn or poppies would follow and the cycle would be repeated (Owens and Clifton, 1972). Altitude has significant effects on the crop calendar of the poppy, so mountain crops mature slightly later than the lowland crops. In the provinces of Helmand and Nangarhar, the opium poppy is planted in the fall, with flowers appearing in late March or early April. After a 2-3 week long flowering stage, the capsule remaining is cut after the fall of the leaves, and then the latex flowing from it is collected every day after oxidation. The poppy harvest stage usually ends 2-3 weeks before the wheat harvest stage begins (Owens and Clifton, 1972).

Among the producers of opium poppy in the world, Afghanistan accounted for approximately 63% of global opium poppy cultivation in 2012, while Myanmar and Laos in South-East Asia accounted for over 20%, and countries in Central America and South America (mainly Mexico and Colombia) accounted for almost 7% (UNODC, 2012). In fact, as shown in Figure 1.3, at least since 1997, Afghanistan has become the biggest and also the dominant opium poppy producer in the world, replacing Myanmar. In terms of poppy cultivation area, Afghanistan has become the dominant country at least since 2004.

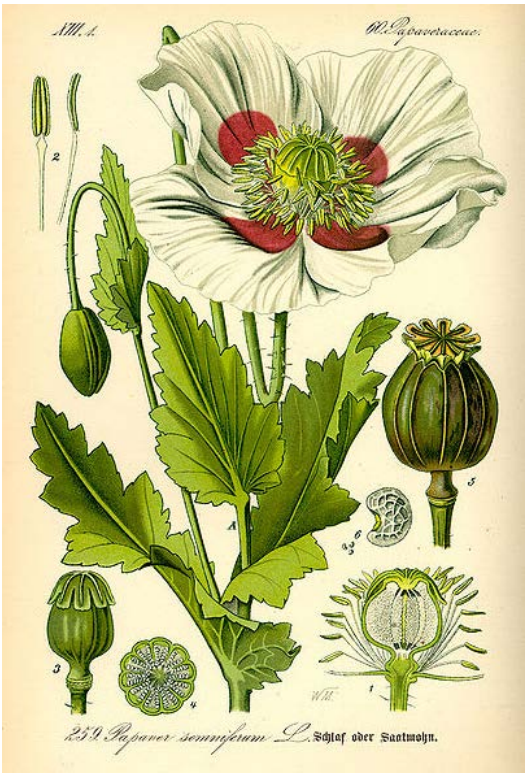

Figure 1.2 Opium Poppy (Source: Otto Wilhelm Thome Flora von Deutschland, Osterreich und der Schweiz 1885, Gera, Germany)

Within Afghanistan, 95% of total opium cultivation took place in the nine provinces in the southern and western regions which are the most insecure due to insurgency and organized criminal networks (UNODC, 2013). Helmand, one of the nine provinces, remained the country's major opium-cultivating province during the past years. It accounted for 49% of the country's total opium cultivation in 2012, 48% of it in 2011, 53% of it in 2010, 57% in 2009, 66% in 2008, 53% in 2007, 42% in 2006, 25% in 2005, 23% in 2004 and 19% in 2003.

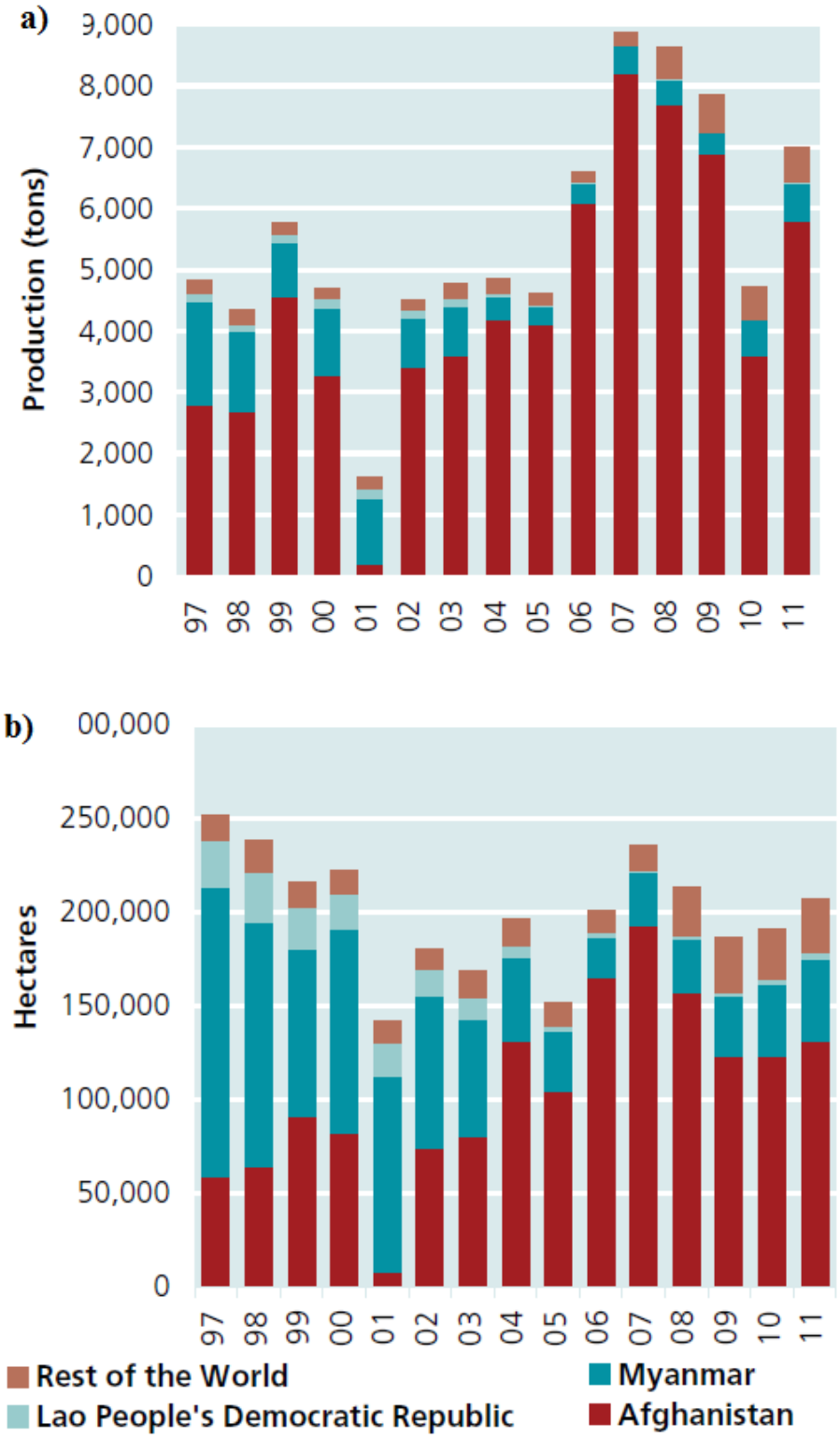

Figure 1.3 Global potential production (a) and illicit cultivation (b) of opium poppy during 1997-2011 (source: World Drug Report 2012)

1.3 Opium Poppy Field Detection in Remote Sensing

Understanding how much drugs are produced is critical to monitoring drug trafficking in the world. However, it is challenging to investigate where and how large opium poppy fields are. Frequent and accurate field surveys are even unfeasible in many regions or countries with bad transportation conditions, insecure environments and other limits.

Satellite remote sensing technology has a great potential for detecting poppy fields because it can overcome the constraints of inaccessible field surveys. In fact, with the recent surge in the availability of spectral imaging sensors, the technology has been widely used for vegetation classification and plant species detection (Langley et al., 2001; Nordberg and Evertson, 2003; Xie et al., 2008).

Remote sensing technologies have also been used to detect poppy fields. However, many problems and limitations still exist. This section reviews the previous studies in order to identify the research gaps. They can be divided into two categories: multispectral data based detection and hyperspectral data based detection.

1.3.1 Studies Using Multispectral Data

The United Nations Office on Drugs and Crime (UNODC) has applied remote sensing techniques to monitor the extent of opium cultivation in Afghanistan since 2002 (UNODC, 2009) due to the increased security difficulties involved in accessing the area. Their work relied on using high spatial resolution satellite multispectral imagery. Their survey design and estimation procedures are introduced below, and more details can be

found in "Afghanistan Opium Survey 2012" (UNODC, 2013) or see UNODC's webpage (http://www.unodc.org/unodc/en/crop-monitoring/index.html) for more references.

In Afghan provinces with a low level of opium cultivation, the target area of a province is fully covered by satellite imagery. However, it is not suitable to use expensive high resolution images for the provinces where poppy crops are planted widely. UNODC uses a sampling approach to cover those provinces. The sampling frame is established by extracting the area of land potentially available for opium cultivation based on Landsat 7 ETM+ images and Disaster Monitoring Constellation (DMC) images. This area is divided into regular 10 km by 10 km grids, which constitute the sampling frame. A certain number of grids are selected randomly to be covered by high spatial resolution images like IKONOS, QuickBird, WorldView-2 and GeoEye images of 1 m resolution and 0.5 m resolution (PAN-sharpened). The total number of images is constrained by availability due to cost considerations, weather conditions and the limited time window for each image (UNODC, 2013).

Opium poppy fields are delineated by visual interpretation of high spatial resolution imagery. UNODC uses a pair of images that are acquired at two stages, namely the pre-harvest (flowering or capsule) stage and the post-harvest (post-lancing) stage. Opium poppy fields are initially identified using first-dated images aided by ground-truth information collected in the form of segment maps, GPS points, field photographs and aerial photographs. Then, the interpretation based on first-dated images is improved by comparing with second-dated images. In addition, to estimate the national area of opium poppy cultivation, UNODC (2013) applies a ratio of poppy area

over potential agricultural land in satellite images, using total potential agricultural land as an auxiliary variable.

Multispectral data were also used in other studies. For instance, Tian et al. (2011) used multispectral data to estimate opium poppy cultivation area in a study area in North Myanmar through auto-classification, visual interpretation and ground verification. The spectral data used included SPOT-5, ALOS and ASTER images with 10–15 m resolution and QuickBird, IKONOS images with even much higher spatial resolution. Therefore, the main sources of used remote sensing multispectral data were the high spatial resolution data in detection of poppy fields.

1.3.2 Studies Using Hyperspectral Data

As hyperspectral data better describe the spectral signatures of targets, a few studies attempted to identify opium poppy from hyperspectral data collected by a spectrometer through laboratory experiments or field spectral surveys. Lowe (2010) carried out a laboratory experiment to measure the spectra of opium and wheat at different growth stages. Based on his measurements, he used vegetation indices such as the Normalized Difference Vegetation Index (NDVI) and the Modified Red Edge Normalized Difference Vegetation Index (MRENDVI) to discriminate between the opium poppy and wheat plots. He indicated that a discrimination of opium poppy and wheat crops can be performed at an optimal phenological phase if these vegetation indices are employed, and the best time depends on time lags between the individual harvest points of opium poppy and wheat.

Jia et al. (2011) investigated whether opium poppy can be spectrally discriminated from coexisting species (e.g., wheat, barley and alfalfa) through field spectrometer measurements at canopy level in an official farm in China. They reported that flowering time was the best time to identify opium poppy from other coexisting species. Nakazawa et al. (2012) measured hyperspectral data of poppy and of wheat in a medical botanical garden and a university farm, respectively in Tokyo, Japan using the FieldSpec Portable Spectroradiometer of Analytical Spectral Devices Inc. (Boulder, Colorado, USA). They reported that poppy fields could be discriminated correctly from wheat fields using red edge position computed from measured hyperspectral data.

No publications have been found in the literature review that used airborne or satellite hyperspectral data for opium field detection.

1.3.3 Research Problem

As mentioned above, the previous studies that used multispectral data depended on high spatial resolution images in detection of poppy fields. These high resolution images are too expensive to cover a huge region like Afghanistan, a developing country, when foreign financial aid is not available.

As to the studies using hyperspectral data to detect poppy fields, they relied on spectral measurements through laboratory experiments or field surveys. Until now, there is little evidence that opium fields have been identified from aerial or satellite hyperspectral images. Airborne hyperspectral imagery is more risky and more difficult to obtain in regions like Afghanistan because of security risks and the remoteness. Moreover, airborne hyperspectral imagery is also costly.

The imagery of EO-1 Hyperion, the only spaceborne hyperspectral sensor currently in operation, is free of charge. But, its spatial resolution is only 30 m × 30 m, which is coarse in relation to the size of poppy fields (about 15 m × 15 m or less to 100 m × 100 m). Therefore, to detect poppy fields using EO-1 Hyperion imagery, the method must be able to detect subpixel targets. In addition, the method must be unsupervised because training samples are extremely difficult to obtain through field surveys under the special circumstances in Afghanistan or in other countries where illegal opium is planted.

Although some classification methods exist that do not require training samples (e.g., Self-Organizing Data Analysis Technique Algorithm (ISODATA) and k-mean clustering algorithms), analysts are required to know the number of classes and assign several parameters including the number of iterations when using these unsupervised methods. ISODATA and k-means are very sensitive to these parameters (Goncalves et al., 2008). Moreover, class splitting, merging and deleting also depend on analysts. All of these factors may introduce considerable subjectivity into the classification process (Lang et al., 2008). This makes these conventional unsupervised methods not suitable for Afghanistan because only very little information about the study area was available.

1.4 Research Objective

The aim of this research was to find a practical and economical way to detect poppy fields from EO-1 Hyperion imagery. To make it suitable for the specific conditions in opium poppy producing regions in Afghanistan, the detection method should be:

- unsupervised, i.e., not require training samples of poppy;
- computationally efficient;
- less site-specific (so, popular advanced methods like artificial neural network-based models cannot perform well, because they are mostly site specific); and
- able to detect poppy fields before harvest in order to timely conduct poppy eradication (so, it cannot use a pair of images that are acquired at two stages, namely the pre-harvest stage and the post-harvest stage to detect poppy fields as UNODC did.).

1.5 Proposed Methodology

This section provided a brief description of the research conducted for accomplishing the objectives of this study. The satellite data used in this research, i.e., EO-1 Hyperion hyperspectral data and ALI multispectral data (both with 30 m ground resolution), were obtained from the United States Geological Survey (USGS) website (http://glovis.usgs.gov/) at no charge. The data pre- and post-processing were implemented mainly using ENVI/IDL and ESRI's ArcGIS software.

In Chapter 2, an unsupervised Multiple Endmember Spectral Mixture Analysis (MESMA)-based method to detect poppy fields was proposed in a study area located in central Helmand Province, Afghanistan from an EO-1 Hyperion hyperspectral image. No training samples of poppy were involved in the process of poppy field detection. Chapter 3 proposed an unsupervised Mixture-Tuned Matched Filtering (MTMF)-based

method to detect the poppy fields from the same Hyperion image in the same study area used in Chapter 2. This MTMF-based method requires much less computational time than the MESMA-based one. It did not require any training samples in detection, too.

In Chapter 4, the MTMF-based method was further tested and validated in another selected study area in mountainous east Afghanistan using another EO-1 Hyperion hyperspectral image acquired in another year. Chapter 5 investigated if poppy fields could be detected using moderate spatial resolution multispectral data, i.e. EO-1 ALI multispectral image, by applying the MTMF-based method. The ALI image was acquired at the same time as the Hyperion image in the same study area used in Chapters 2 and 3.

1.6 Overview of Each Chapter

This thesis was organized into six chapters. Chapter 1 introduced briefly the opium poppy and its production, and then reviewed previous studies on remote sensing for poppy field detection. The identified research gaps were used to determine the research objective of this thesis. The general methodological design and the thesis structure were also introduced.

Chapters 2 and 3 proposed two unsupervised methods (a MESMA-based, and a MTMF-based) to detect poppy fields in central Helmand Province, southwest Afghanistan from a Hyperion image. In Chapter 4, the MTMF-based method was tested in mountainous east Afghanistan using another Hyperion image. In addition, Chapter 5 found that EO-1 ALI multispectral data could not detect poppy fields reliably.

The final Chapter, Chapter 6, summarized and concluded the research presented in this thesis, and highlighted the contributions of this thesis towards the research objective. Then, recommendations for further research were presented.

References

Goncalves, M.L., M.L.A. Netto, J.A.F. Costa, and J.Z. Junior (2008) "An unsupervised method of classifying remotely sensed images using Kohonen self-organizing maps and agglomerative hierarchical clustering methods." *International Journal of Remote Sensing*, Vol. 29, No. 11, pp. 3171-3207.

Jia, K., B. Wu, Y. Tian, Q. Li, and X. Du (2011). "Spectral discrimination of opium poppy using field spectrometry." *IEEE Transactions on Geoscience and Remote Sensing*, Vol. 49, No. 9, pp. 3414-3422.

Lang, R., G. Shao, B.C. Pijanowski, and R.L. Farnsworth (2008) "Optimizing unsupervised classifications of remotely sensed imagery with a data-assisted labeling approach." *Computers & Geosciences*, Vol. 34, pp. 1877–1885.

Langley, S.K., H.M. Cheshire, and K.S. Humes (2001) "A comparison of single date and multitemporal satellite image classifications in a semi-arid grassland." *Journal of Arid Environments*, Vol. 49, pp. 401–411.

Lowe, A. (2010). "Remote Sensing based Monitoring of Opium Cultivations in Afghanistan." Master dissertation, University of Bonn, 106 p.

Nakazawa, A., J.H. Kim, T. Mitani, S. Odagawa, T. Takeda, C. Kobayashi, and O. Kashimura (2012). "A study on detecting the poppy field using hyperspectral remote sensing techniques." 2012 IEEE International Geoscience and Remote Sensing Symposium (IGARSS), 22-27 July 2012, Munich.Page(s): 4829 - 4832 (DOI: 10.1109/IGARSS.2012.6352532).

Nordberg, M.L., and J. Evertson (2003) "Vegetation index differencing and linear regression for change detection in a Swedish mountain range using Landsat TM and ETM+ imagery." *Land Degradation & Development*, Vol. 16, pp. 139–149.

Owens, G.P., and J.H. Clifton (1972). "Poppies in Afghanistan." USAID - Kabul, Afghanistan, 34 p.

Sader, S.A. (1991). "Remote Sensing of Narcotic Crops with special reference to techniques for detection and monitoring of poppy production in Afghanistan." [Online] June 9, 2013: http://pdf.usaid.gov/pdf_docs/PNABT431.pdf.

Tian Y.C., B.F. Wu, L. Zhang, Q.Z. Li, K. Jia, and M.P. Wen (2011). "Opium poppy monitoring with remote sensing in North Myanmar." *International Journal of Drug Policy*, Vol. 22, pp. 278–284.

UNODC (2012). "World Drug Report 2012." [Online] July 27, 2013: http://www.unodc.org/documents/data-and-analysis/WDR2012/WDR_2012_web_small.pdf.

UNODC (2013). "Afghanistan Opium Survey 2012." [Online] July 27, 2013: http://www.unodc.org/documents/crop-monitoring/Afghanistan/ORAS_report_2012.pdf.

Wikipedia (2013). "Papaver somniferum." [Online] July 10, 2013: http://en.wikipedia.org/wiki/Papaver_somniferum.

Xie, Y. (2008) "Remote sensing imagery in vegetation mapping: A review." *Journal of Plant Ecology*, Vol. 1, No. 1, pp. 9-23.

CHAPTER 2

REMOTE SENSING OF OPIUM POPPY FIELDS USING EO-1 HYPERION HYPERSPECTRAL DATA: AN EXAMPLE IN AFGHANISTAN

* This paper is coauthored by Wang, J.J., Zhang, Y. and Bussink, C., and it is a revised version of a published international conference paper and referred as:

Wang, J.J., Y. Zhang, and C. Bussink (2013) "Remote Sensing of Opium Poppy Fields Using EO-1 Hyperion Hyperspectral Data: an Example in Afghanistan." Proceedings of the 2013 Canadian Institute of Geomatics Annual Conference and the 2013 International Conference on Earth Observation for Global Changes (EOGC'2013), 5-7 June 2013, Toronto, Ontario, Canada, pp. 106-110.

Abstract

Each year, the global use of opium and its derivatives like heroin take the lives of thousands of people. There is a very high chance that the source material for these drugs comes from Afghanistan, the primary illicit opium producer in the entire world. It is crucial to monitor opium poppy cultivation. However, *in situ* detection of opium poppy fields is often expensive, time-consuming and even quite dangerous in some regions like Afghanistan. To overcome the constraints of inaccessibility of poppy fields, high-resolution ($\leq$ 1m) images like pan-sharpened IKONOS have been applied by some organizations such as United Nations Office on Drugs and Crime that has been monitoring the extent of the problem for more than a decade. Unfortunately, these high-resolution images are expensive, especially when they are used to monitor a huge area

and despite the use of sampling approaches. In contrast, less expensive medium spatial resolution satellite hyperspectral data provide almost continuous spectra of targets and backgrounds, which may increase the detection capability of subpixel size targets. However, until now, little research was found that identified opium fields from spaceborne or aerial hyperspectral images. Therefore, this study applied an EO-1 Hyperion hyperspectral image, which is free of charge, to detect poppy fields in a study area located in Southwest Afghanistan. It was found that, by using a methodology that was based on unsupervised endmember-selection and multiple-endmember spectral mixture analysis, poppy fields could be detected directly from the Hyperion image, and the number of poppy pixels was overestimated by 12%.

Keywords: Opium poppy field, EO-1 Hyperion, Hyperspectral data, Target detection, MESMA, Helmand, Afghanistan

2.1 Introduction

Each year, opium makes tens of thousands of people lose their lives; meanwhile, opium also leads to poverty as well as other serious social problems worldwide. Since 1992, Afghanistan, replacing the Golden Triangle region of Southeast Asia, has gradually become the primary illicit opium producer of opium in the entire world. The potential productions of opium in Afghanistan represented 88%, 74% and 82% of global

potential opium production in 2009, 2010 and 2011, respectively (UNODC, 2011; UNODC, 2012).

In order to effectively fight against the opium production, it is necessary to timely and accurately investigate where the opium poppy fields. However, monitoring opium fields is often an extremely difficult and even quite dangerous task, especially in the regions with bad transportation conditions and insecure environments. In these regions, frequent and accurate field surveys are often unfeasible.

To overcome the constraints of inaccessibility of field surveys, satellite remote sensing with wide spatial coverage, high temporal repeatability and increasing spatial resolutions, may provide an alterative option to do this job possibly. For instance, remote sensing technologies have been applied by the United Nations Office on Drugs and Crime (UNODC) to monitor the extent of opium cultivation in Afghanistan since 2002 (UNODC, 2009). High-resolution ($\leq$ 1m) pan-sharpened IKONOS, QuickBird, WorldView-2 and GeoEye images were visually interpreted to identify opium fields as well as to verify opium poppy eradication. These high resolution images have also been used in other studies to detect poppy production (e.g., Taylor et al., 2010; Tian et al., 2011). However, these high-resolution multispectral images are expensive, especially when they are used to monitor a large area such as Afghanistan.

EO-1 Hyperion images, the only available satellite hyperspectral data, are free of charge. Their spatial resolution is coarse (30m). But, the hyperspectral data having hundreds of channels with spectral interval of around 10 nm provide almost continuous spectra of targets and natural backgrounds, and this may increase the detection capability

of subpixel size targets (Manolakis, 2002). However, until now, little research can be found that identified opium fields from satellite or aerial hyperspectral images. Currently, only a few studies attempted to identify opium poppy from other crops using the hyperspectral data that were collected by a hand-held spectrometer in laboratory (Lowe, 2010) or in official farms (Jia et al., 2011; Nakazawa et al., 2012). It was reported that opium poppy's spectral characters varied with different growth periods (Lowe, 2010; Jia et al., 2011), and around flowering time was the best time to identify opium poppy from other coexisting species (Jia et al., 2011). Nevertheless, compared with these laboratory experiments and field spectral surveys, which are controllable to some extent, it is much more complex and difficult when real remote sensing images are applied to detect poppy fields.

This study aimed to detect poppy fields from free EO-1 Hyperion hyperspectral imagery. As the spatial resolution of Hyperion data was coarse (30 m × 30 m) relative to the size of poppy fields (about 15 m × 15 m or less to 100 m × 100 m) in Afghanistan, spectral unmixing had to be conducted to detect subpixel size target. This study selected the spectral mixture analysis (SMA) approach of Multiple Endmember Spectral Mixture Analysis (MESMA; Roberts et al., 1998). The MESMA is the most widely used spectral unmixing technique, and its capability to account for variable endmembers (see Appendix I) has been successfully tested in natural, urban and extraterrestrial environments using both multi- and hyperspectral optical, and thermal imagery (Somers et al., 2011). Other potential difficulties included the lack of opium poppy’s spectra in current various spectral libraries such as United States Geological Survey (USGS) Digital Spectral Library and ASTER spectral library, the lack of in situ information used

as training data, the lack of in-situ atmospheric condition data for atmospheric correction, etc.

2.2 Study Area and Materials

2.2.1 Study Area

The selected study area in the central Helmand Province was on the arid plateau in southwest Afghanistan (Figure 2.1). According to "Afghanistan Opium Survey 2011" (UNODC, 2011), Helmand is the dominant opium cultivating province, and the cultivation area was 63,307 ha, and 48% of the total opium cultivation area of the country in 2011. This province alone produced 52% of all Afghan opium in 2011. Meanwhile, Helmand was one of the most insecure provinces in this country, so field monitoring was quite dangerous.

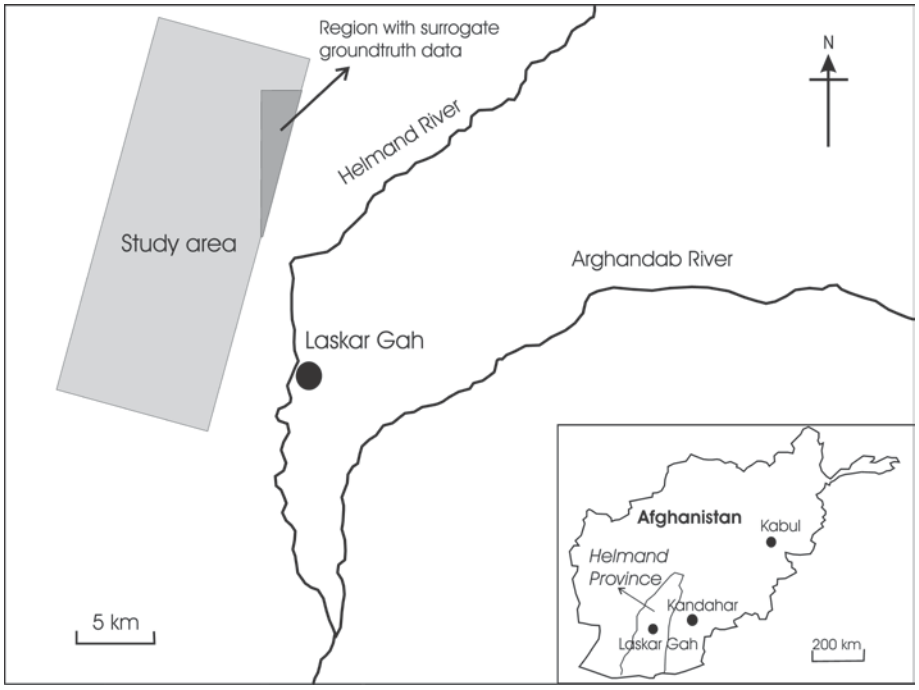

Figure 2.1 Study area

2.2.2 Materials

Interpretation files of opium fields were provided by the UNODC for the research area. The interpretations were based on an IKONOS image acquired on April 11, 2009, before harvest season. The interpretations were used as surrogate groundtruth in this study.

An EO-1 Hyperion hyperspectral image over the study area acquired on March 11, 2009, a pre-harvest date, was applied in this study. The image was at level L1R processing, meaning that it was radiometrically but not geometrically corrected. In addition, to geometrically correct the Hyperion image, a Landsat ETM+ image acquired on April 23, 2009 was applied.

2.3 Methodology

There exist a number of approaches to perform endmember selection and spectral unmixing (Somers et al., 2011; Linn et al., 2010). This study proposed a methodology that was based on unsupervised endmember-selection and multiple-endmember SMA to detect poppy fields. A complete methodology work flow for this paper is shown in Figure 2.2. The detection accuracy was assessed by comparing the results, pixel by pixel, with the surrogate ground truth data of poppy field provided by UNODC.

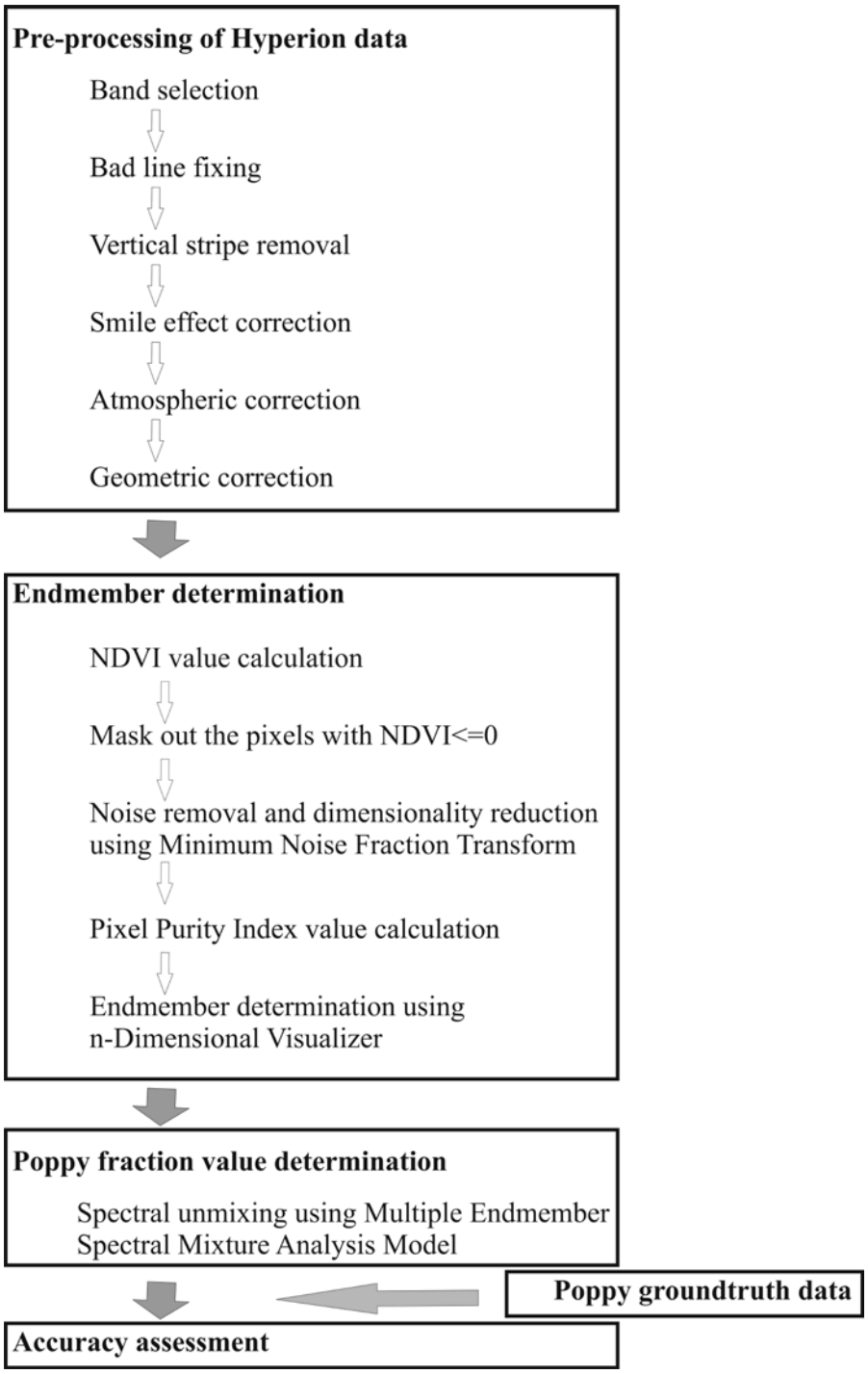

Figure 2.2 Methodology workflow

2.3.1 Hyperion Hyperspectral Data Pre-processing

Hyperion data contain 242 spectral bands in total, 44 ones of which are not calibrated because they are intentionally not illuminated or correspond to areas of low sensitivity of the spectrometer materials (Datt et al., 2003). Among the other 198 bands, only 196 bands are unique (bands 8-57 and 79-224) because there are four bands in the overlap between the two spectrometers of VNIR and SWIR (Datt et al., 2003). In addition, atmospheric water vapor bands which absorb almost the entire incident and reflected solar radiation and the bands that have very severe vertical stripping were identified by visual inspection of the image data (Beck, 2003). Thus, the subset of 121 selected bands (bands 8-56, 79-119, 135-164, and 195 within 426.8-2102.9 nm) was applied in this study.

For the subset of 121 selected bands, bad lines that have lower DN values as compared to their neighboring pixels were corrected by replacing their DN values with the average DN values of their immediate left and right neighboring pixels (Han et al., 2002). Vertical stripes were removed using the local destriping method presented in Datt et al. (2003). The "smile effects" that refer to an across-track wavelength shift from center wavelength due to the change of dispersion angle with field position (Goodenough et al., 2003) were removed using the procedure of "Cross-Track Illumination Correction" (Jupp et al., 2003) in the ENVI software (ITT Visual Information Systems, 2006). The correction of "smile effect" was checked by Minimum Noise Fraction (MNF) transform because "smile effect" can lead to a brightness gradient appearing in the first eigenvalue image after MNF transform (Green et al., 1988; Goodenough et al., 2003).

This study used Fast Line-of-sight Atmospheric Analysis of Spectral Hypercubes (FLAASH), an atmospheric correction module implemented in the ENVI to calibrate the at-sensor radiance data to land surface reflectance. As Hyperion level L1R data are in units of $W/(m^2\ \mu m\ sr)\times 40$ for the VNIR or $\times 80$ for the SWIR while the FLAASH atmospheric correction software uses units of $\mu W/(cm^2\ nm\ sr)$, the scale factors 10 were used when running the FLAASH model (Beck, 2003).

The Hyperion image used was at Level 1R (L1R), so geometric correction was required. The atmospherically corrected image was projected to UTM 41N, datum WGS 84 first. Then, geometric correction was conducted on the Hyperion image by using the georeferencing tool in ArcMap (ESRI Inc., Redlands, California) and collecting 16 ground control points (GCPs) in reference to the Landsat 7 ETM+ imagery acquired on April 23, 2009 over the study area. An overall root mean square error (RMSE) of 7.06 m was achieved.

2.3.2 Endmember Determination

An endmember refers to a spectrally pure pixel. A component may have various endmembers, or various endmember spectral signatures (e.g., poppy component may have various poppy endmembers), caused by spatial and temporal variability in the condition of scene components and differential illumination conditions (Somers et al., 2011).

A mixed pixel may include various endmembers. The following procedures of hyperspectral analysis were employed, including the MNF transform for reducing

spectral data, the Pixel Purity Index (PPI) for identifying those spectrally pure pixels, and the n-Dimensional Visualizer for determining the main components.

First, Normalized Difference Vegetation Index (NDVI) values were computed from Band 31 (660.85 nm) and Band 44 (793.13 nm) for each pixel. Only the pixels with NDVI values greater than 0 were used in further analysis because the other pixels could be seen as “water pixels”. This study used the MNF transform to determine the inherent dimensionality of image data, and to segregate noise in the data (Boardman and Kruse, 1994). The inherent dimensionality of the data is determined by examining the final eigenvalues and the associated images. In this study, only the first six MNF bands with high eigenvalues were used in following stages because the other MNF bands with low eigenvalues carried more noises.

Then, PPI values were computed from the MNF output by using the ENVI software. Higher PPI values represented the pixels with higher purity and spectral extremity. The most spectrally pure pixels typically correspond to mixing endmembers. Separating purer pixels from more mixed pixels benefited separation and identification of endmembers. In this study, only the pixels with PPI values not less than 2000 were used in the following steps. Among them, the pixels whose NDVI values were greater than 0.2 and less than 0.3 were also not involved in further analysis, because they were mixed pixels of non-vegetation and vegetation according to their spectra. The 47 pixels whose NDVI values were greater than 0 and less than 0.2 were seen as non-vegetation pixels (Tsai et al., 2007; Noujdina and Ustin, 2008). The other 31 pixels were input into the n-Dimensional Visualizer in ENVI for the clustering process, which clustered the 31 pixels into two distinct groups (Figure 2.3) representing two kinds of vegetations as

shown in Figure 2.4. The two main crops were poppy and wheat at the season in the study area in 2009, and poppy had lower NDVI value than wheat (UNDOC, 2009; Lowe, 2010). Component A should be poppy because its NDVI was 0.77, lower than Component B whose NDVI value was 0.85. All the 10 vegetation pixels in Component A, 21 vegetation pixels in Component B as well as the 47 non-vegetation pixels were saved into three regions of interest (ROIs) to determinate fraction images in the following steps.

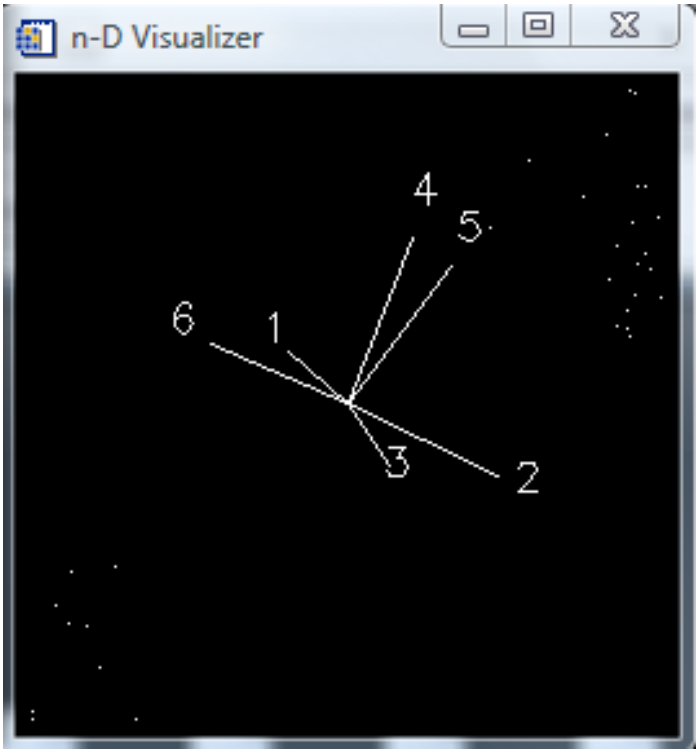

Figure 2.3 The 31 pure vegetation pixels formed two distinct vegetation clusters, Components A (bottom left) and B (top right) in the n-Dimensional Visualizer in ENVI. The numbers referred to MNF band numbers.

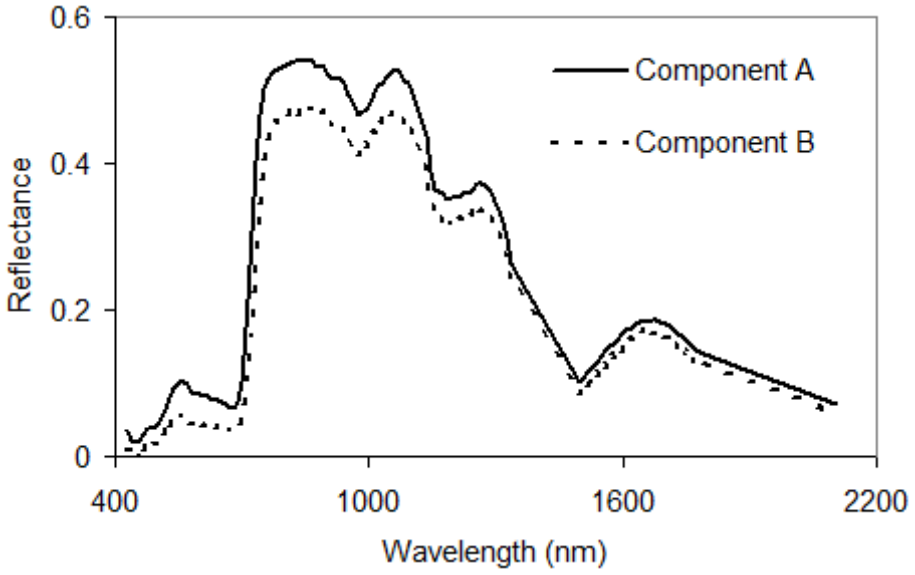

Figure 2.4 Spectral profile of averaged reflectance of endmembers in the two vegetation clusters, i.e., Components A and B, respectively.

2.3.3 Poppy Fraction Value Determination

To account for the great spectral heterogeneity in the study area, this study applied the MESMA (Roberts et al., 1998) to perform spectral unmixing. This model permits multiple endmembers for each component and thereby refutes the fixed endmember restriction made in traditional simple SMA (sSMA; Somers et al., 2011). The MESMA model accounts for each plausible endmember condition in an iterative procedure, so that it may assign the best-fit model (i.e., lowest RMSE) to each pixel.

This study used the 'Create Spectral Library from ROIs' module in the free software package "VIPER Tools" (Roberts et al., 2007) to build a spectral library from the three ROIs created in the above step for each endmember of each component to preserve spectral diversity, rather than used simple averages of all pixels within a ROI.

Then, the MESMA model was implemented to produce the fraction image poppy using the mixing tools in the “VIPER Tools” software. In addition, in order to compare with the result produced using multiple endmembers, this study also used an averaged endmember of each component to produce the fraction image of poppy by using sSMA.

This study applied two, three and four endmember MESMA models to the Hyperion data using the “Run SMA/MESMA” module of VIPER Tools (Table 2.1), respectively. For instance, 4-endmember model referred that one of endmembers of the poppy component, one of endmembers of the wheat component, one of endmembers of the non-vegetation component as well as shade were used to conduct spectral unmixing in each iteration. As to the required restriction parameters, this study used the default values. Namely, the minimum allowable fraction, maximum allowable fraction, maximum allowable shade fraction, maximum allowable RMSE, residual threshold and number of contiguous bands were -6%, 106%, 80%, 0.025, 0.025 and 7, respectively. The photometric shade (zero reflectance) was used.

Because the spectral signatures are quite similar between poppy and wheat, this study added a restriction parameter. If the RMSE difference of reflectance was greater than 0.05% between two models, the pixel was modelled by the model with lower RMSE. Otherwise, the pixel was not modelled.

This study applied 2-, 3- and 4-endmember MESMA models to each pixel. If a 2-endmember solution is satisfactory, a pixel will be unmixed with the two endmembers. If unsatisfactory, the pixels will then be unmixed with a 3-endmember solution. Then, if a 3-endmember solution is satisfactory, a pixel will be unmixed with the three

endmembers. If unsatisfactory, the pixels will then be unmixed with four endmembers. Thus, the fraction image of poppy could be determined.

Table 2.1 Number of MESMA models used

Number of endmembers	1st endmember	2nd endmember	3rd endmember	4th endmember	Number of models
2	poppy	shade			10
2	wheat	shade			21
2	non-vegetation	shade			47
3	poppy	wheat	shade		210
3	poppy	non-vegetation	shade		470
3	wheat	non-vegetation	shade		987
4	poppy	wheat	non-vegetation	shade	9870

2.4 Results and Discussion

Three poppy field distribution maps were retrieved through using MESMA with 2-, 3- and 4-endmember models, MESMA with only 2- and 3-endmember models, and sSMA with only 2- and 3-endmember models, respectively. The retrieved poppy field

distribution maps had two classes, i.e., poppy pixels and non-poppy pixels. These distribution maps were compared, pixel by pixel, against the surrogate groundtruth data provided by UNODC to calculate producer's, user's and overall accuracies, as well as kappa coefficient for accuracy assessment (Table 2.2).

Table 2.2. Comparison of detection accuracies of poppy pixels. The “em” refers to “endmember”.

Detection accuracies of poppy pixels	MESMA (2em & 3em & 4em)	MESMA (2em & 3em)	sSMA (2em & 3em)
Producer's (%)	83	70	12
User's (%)	58	63	72
Overall (%)	71	73	64
kappa	0.42	0.43	0.11

It can be seen from Table 2.2 that, when 2-, 3- and 4-endmember MESMA models were used, only 58% of the detected poppy pixels were really poppy pixels although 83% of true poppy pixels were detected. When only 2- and 3-endmember MESMA models were used, a higher percentage (63%) of the detected poppy pixels were really poppy pixels although a lower percentage (70%) of true poppy pixels were detected. The overall accuracy and kappa coefficient increased, too. This suggested that involving 4-endmember model could detect more poppy pixels, but the detection accuracy was lower. In fact, of the pixels that were modelled as poppy, if using 2-, 3- and 4-endmember models, but modelled as non-poppy pixels, if using 2- and 3-endmember models, only as low as 41% were true poppy pixels in this study. Therefore, the MESMA-based

methodology using 2- and 3-endmember models was selected for detection of poppy fields in the study area.

Some previous studies used 4-endmember MESMA models (e.g., Michishita et al., 2012; Liu and Yang, 2013; Thorp et al., 2013). Powell (2006) and Powell and Roberts (2008) indicated that natural systems were best modelled by two endmembers while disturbed regions required 3-endmember models and urban areas required 4-endmember models generally. This was consistent with the present study.

In addition, this study used MESMA to conduct spectral unmixing. For comparison, a sSMA was also used to conduct spectral unmixing. The averaged endmembers of each component were used. As shown in Table 2.2., when only an averaged endmember was used, the user's accuracy increased to 72%, but only 12% of true poppy pixels were detected. The kappa coefficient (0.11) only indicated a slight agreement between retrieved poppy pixels and groundtruth data. In reality, spectral signatures of the same material or component can vary largely in an image. However, sSMA does not account for such significant spectral variations. In contrast, MESMA allows endmembers to vary on a per-pixel basis (Roberts et al., 1998) within the same material. This may explain why the MESMA performed better in this study.

In addition, as mentioned above, this study introduced a restriction parameter in the proposed MESMA-based methodology in order to select the best model when detecting poppy pixels. This was because the spectral signatures were quite similar between poppy and wheat. If the RMSE difference of reflectance was greater than 0.05% between two models, the pixel was modelled by the model with lower RMSE.

Otherwise, the pixel was not modelled. For instance, a pixel was modelled by the poppy-(non-vegetation)-shade model only when [the RMSE caused by the "poppy-(non-vegetation)-shade" model + 0.05%] was lower than the RMSE caused by the "wheat-(non-vegetation)-shade" model. It was found that, without the restriction of such a threshold, the user's accuracy, overall accuracy and kappa coefficient decreased significantly although more poppy pixels could be detected (Table 2.3). Therefore, this study applied this threshold of RMSE difference in detection of poppy fields in the study area.

Table 2.3. Comparison of detection accuracies of poppy pixels when threshold of RMSE difference (i.e., >0.05%) was used against when no RMSE was used. The MSEMA-based methodology with 2- and 3-endmember models was applied to detect poppy fields.

Detection accuracies of poppy pixels	With threshold (RMSE difference > 0.05%)	Without threshold
Producer's (%)	70	78
User's (%)	63	59
Overall (%)	73	70
kappa	0.43	0.41

Thus, this study derived the distribution map of poppy fields (Figure 2.5(a)) through the MESMA-based methodology using 2- and 3-endmember models. This map clearly showed the poppy fields on March 11, 2009 in the study area. Surrogate groundtruth data of poppy (poppy interpretation files) (see Figure 2.5(c1)) were

available for the subarea within the box “b1”, which showed highly similar to its counterpart (Figure 2.5(b1)) retrieved in this study. This was also supported by the comparison between them for an enlarged part (i.e., Figure 2.5(b2) with Figure 2.5(c2)).

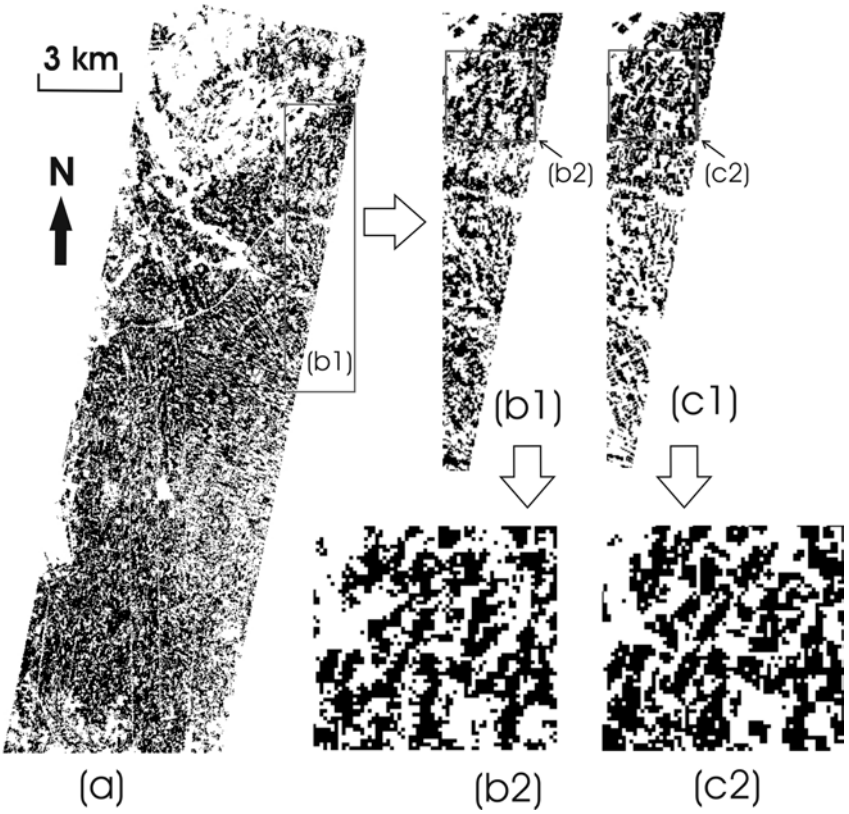

Figure 2.5 Poppy distribution map (a) retrieved from an EO-1 Hyperion image over the study area acquired on March 11, 2009. Surrogate groundtruth map of poppy (c1, and its subset c2) only covering the area within the box “b1” was compared with counterpart (b1, and its subset b2). Black pixels referred to poppy fields.

Accuracy assessment quantified how well poppy detection was done by the MESMA-based methodology. This produced producer's, user's and overall accuracies of 70%, 63% and 73%, respectively, and kappa coefficient of 0.43 which indicated a moderate agreement. The number of poppy pixels was overestimated by 12%. These

demonstrated the potential of the methodology in detection of poppy fields in the study area.

2.5 Conclusions

Timely detection of opium poppy fields from satellite images is important as opium has led to serious social problems worldwide. Previous studies heavily relied on high spatial solution imagery, but the imagery is too expensive for detection of poppy fields in a huge area like Afghanistan where there are significant financial constrains. To detect poppy fields in a study area located in central Helmand, Afghanistan, this study employed EO-1 Hyperion hyperspectral imagery. This is because it was free of charge, and meanwhile its large number of bands benefited detecting subpixel size targets through spectral unmixing.

This study proposed a MESMA-based methodology to detect poppy fields in the study area. In this methodology, MESMA, rather than sSMA, was selected to conduct spectral unmixing because it led to higher detection accuracies in this study. It was found that the MESMA-based methodology performed better when using 2- and 3-endmember models than when using 2-, 3- and 4-endmember models for detection of poppy fields in the study area. In addition, this study found that introducing a restriction parameter (i.e., the RMSE difference of reflectance > 0.05% between two models) in the methodology significantly increased user's accuracy, overall accuracy and kappa coefficient of poppy field detection. The retrieved distribution map of poppy fields looked quite similar to the surrogate groundtruth data, which demonstrates the potential

of this MESMA-based methodology in poppy field detection even when the imagery used had coarse spatial resolution and low signal-to-noise ratio.

Importantly, the proposed MESMA-based methodology jointly applied MNF, PPI and n-Dimensional Visualizer techniques to select endmembers of main components from the image itself. It was unsupervised, and did not require any training samples to detect poppy fields in the study area. Meanwhile, analysts just needed to account for endmembers of main, rather than all, vegetation components in a landscape. Conventional methods cannot work effectively in the study area because it is often dangerous, or even unfeasible sometime to obtain enough in situ information to use as training data in detection due to security reasons.

A number of factors may affect the detection accuracies of poppy fields from EO-1 Hyperion imagery. For instance, spectral signatures of plants may vary at different growth stages. Different geomorphologic environmental may affect atmospheric correction, and good atmospheric correction is critical for target detection. Different coexisting vegetations with poppy may also affect the detection of poppy fields. Therefore, this MESMA-based methodology will be further tested in future research. More study areas located in different environments in Afghanistan will be involved.

Acknowledgements

This work was supported by the Canada Research Chairs Program. The authors thank the United Nations Office on Drugs and Crime (UNODC) for providing the interpretation files of opium fields. The views expressed in this paper are those of the author(s) and do not necessarily reflect the views of the United Nations.

References

Beck, R. (2003). "EO-1 User Guide v.2.3." [Online] October 17, 2012: http://eo1.usgs.gov/documents/EO1userguidev2pt320030715UC.pdf.

Boardman, J. W., and F.A. Kruse (1994). "Automated spectral analysis: A geologic example using AVIRIS data, north Grapevine Mountains, Nevada." *Proceedings, Tenth Thematic Conference on Geologic Remote Sensing*, Environmental Research Institute of Michigan, Ann Arbor, MI, p. I-407 - I-418.

Datt, B., T.R. McVicar, T.G. Van Niel, D.L.B. Jupp, and J.S. Pearlman (2003). "Preprocessing EO-1 Hyperion Hyperspectral Data to Support the Application of Agricultural Indexes." *IEEE Transactions on Geoscience and Remote Sensing*, Vol. 41, No. 2, pp. 1246-1259.

Goodenough, D.G., A. Dyk, K.O. Niemann, J.S. Pearlman, H. Chen, T. Han, M. Murdoch, and C. West (2003). "Processing Hyperion and ALI for forest classification," *IEEE Transactions on Geoscience and Remote Sensing*, Vol. 41, pp. 1321-1331.

Green, A.A., M. Berman, P. Switzer, and M.D. Craig (1988). "A transformation for ordering multispectral data in terms of image quality with implications for noise removal." *IEEE Transactions on Geoscience and Remote Sensing*, Vol. 26, pp. 65-74.

Han, T., D.G. Goodenough, A. Dyk, and J. Love (2002). "Detection and correction of abnormal pixels in Hyperion image." *IEEE International Geoscience and Remote Sensing Symposium*, vol. III, Toronto, ON, Canada, 1327–1330.

Jia, K., B. Wu, Y. Tian, Q. Li, and X. Du (2011). "Spectral discrimination of opium poppy using field spectrometry." *IEEE Transactions on Geoscience and Remote Sensing*, Vol. 49, No. 9, pp. 3414-3422.

Jupp, D.L.B., B. Datt, T.R. McVicar, T.G. Van Niel, J.S. Pearlman, J.L. Lovell, and E.A. King (2003). "Improving the analysis of Hyperion red-edge index from an agricultural area." *Proceedings of SPIE*, Vol. 4898, pp. 1-15.

Linn, R.M., S.B.A. Rolim, and L.S. Galvao (2010). "Assessment of the multiple endmember spectral mixture analysis (MESMA) model applied to the Hyperion/EO-1 hyperspectral data of the coastal plain of Rio Grande Do Sul, Brazil." In: Wagner W., Szekely, B. (eds.): *ISPRS TC VII Symposium – 100 Years ISPRS*, Vienna, Austria, July 5–7, 2010, IAPRS, Vol. XXXVIII, Part 7A.

Liu, T., and X.J. Yang (2013). "Mapping vegetation in an urban area with stratified classification and multiple endmember spectral mixture analysis." *Remote Sensing of Environment*, Vol. 133, pp. 251–264.

Lowe, A. (2010). "Remote Sensing based Monitoring of Opium Cultivations in Afghanistan." Master dissertation, University of Bonn, 106 p.

Manolakis, D. (2002). "Detection Algorithms for Hyperspectral Imaging Applications," *Project Report HTAP-8*, Lincoln Labs, Massachusetts Institute of Technology, Lexington Massachusetts.

Michishita, R., Z. Jiang, and B. Xu (2012). "Monitoring two decades of urbanization in the Poyang Lake area, China through spectral unmixing." *Remote Sensing of Environment*, Vol. 117, pp. 3–18.

Nakazawa, A., J.H. Kim, T. Mitani, S. Odagawa, T. Takeda, C. Kobayashi, and O. Kashimura (2012). "A study on detecting the poppy field using hyperspectral remote sensing techniques." 2012 IEEE International Geoscience and Remote Sensing Symposium (IGARSS), 22-27 July 2012, Munich.Page(s): 4829 - 4832 (DOI: 10.1109/IGARSS.2012.6352532).

Noujdina, N.V., and S.L. Ustin (2008). "Mapping Downy Brome (Bromus tectorum) using multidate AVIRIS data." *Weed Science*, Vol. 56, pp. 173–179.

Powell, R.L. (2006). "Long-Term Monitoring of Urbanization in the Brazilian Amazon Using Remote Sensing." PhD dissertation, University of California, Santa Barbara, 257p.

Powell, R.L., and D.A. Roberts (2008). "Characterizing variability of the urban physical environment for a suite of cities in Rondonia, Brazil." *Earth Interactions*, Vol. 12, pp. 1−32.

Roberts, D.A., M. Gardner, R. Church, S. Ustin, G. Scheer, and R.O. Green (1998). "Mapping Chaparral in the Santa Monica Mountains using Multiple Endmember Spectral Mixture Models." *Remote Sensing of Environment*, Vol. 65, pp. 267−279.

Roberts, D.A., K. Halligan, and P.E. Dennison (2007). "VIPER Tools User Manual." Version 1.5, [Online] November 20, 2012: www.vipertools.org.

Somers, B., G.P. Asner, T. Laurent, and P. Coppin (2011). "Endmember variability in Spectral Mixture Analysis: A review." *Remote Sensing of Environment*, Vol. 115, No. 7, pp. 1603-1616.

Taylor, J.C., T.W. Waine, G.R. Juniper, D.M. Simms, and T.R. Brewer (2010). "Survey and monitoring of opium poppy and wheat in Afghanistan: 2003-2009." *Remote Sensing Letters*, Vol. 1, No. 3, pp. 179–185.

Thorp, K.R., A.N. French, and A. Rango (2013). "Effect of image spatial and spectral characteristics on mapping semi-arid rangeland vegetation using multiple endmember spectral mixture analysis (MESMA)." *Remote Sensing of Environment*, Vol. 132, pp. 120–130.

Tian Y.C., B.F. Wu, L. Zhang, Q.Z. Li, K. Jia, and M.P. Wen (2011). "Opium poppy monitoring with remote sensing in North Myanmar." *International Journal of Drug Policy*, Vol. 22, pp. 278–284.

Tsai, F., E.-K. Lin, and K. Yoshino (2007). "Spectrally segmented Principal Component Analysis of hyperspectral imagery for mapping invasive plant species." *International Journal of Remote Sensing*, Vol. 28, pp. 1023–1039.

UNODC (2009). "Afghanistan Opium Survey 2009." [Online] October 16, 2012: http://www.unodc.org/documents/crop-monitoring/Afghanistan/Afgh-opiumsurvey2009_web.pdf.

UNODC (2011). "Afghanistan Opium Survey 2011." [Online] October 16, 2012: http://www.unodc.org/documents/crop-monitoring/Afghanistan/Afghanistan_opium_survey_2011_web.pdf.

UNODC (2012). "World Drug Report 2012." [Online] July 27, 2013: http://www.unodc.org/documents/data-and-analysis/WDR2012/WDR_2012_web_small.pdf.

CHAPTER 3

AN UNSUPERVISED MTMF-BASED METHOD FOR DETECTING OPIUM POPPY FIELDS IN HELMAND, AFGHANISTAN, FROM EO-1 HYPERION DATA

* This paper is coauthored by Wang, J.J., Zhang, Y. and Bussink, C., and it has been submitted to *International Journal of Remote Sensing*.

Abstract

Remote sensing has special advantages to monitor the extent of the drug production that causes serious problems to the global society. Although remote sensing has been used to monitor opium poppy fields, the main employed data have been high-resolution images (≤ 1 m) like pan-sharpened IKONOS, QuickBird, etc. These images are costly, making the full coverage of the crop fields in a large area an expensive exercise. As an alternative, the imagery acquired by EO-1 Hyperion, the only available spaceborne hyperspectral sensor currently, is free. However, its spatial resolution is coarser (30 m). Until now, there is little evidence that poppy fields have been identified from aerial or satellite hyperspectral images. This study proposed an unsupervised Mixture Tuned Matched Filtering (MTMF)-based method to detect poppy fields from a Hyperion image covering a study area in Helmand, Afghanistan. This method requires neither training samples nor a preset class number as such information is extremely

difficult to obtain through field surveys. In addition, an accuracy improvement was achieved by considering the pixels with zero or negative matched filtering (MF) scores into the process, unlike the commonly recommended approaches where these pixels were ignored. The retrieved poppy field distribution map showed significant agreement with surrogate groundtruth data. The resultant producer's, user's, overall accuracies and kappa coefficient were 61%, 73%, 76% and 0.48, respectively. The number of derived poppy pixels covered 83% of the number of real poppy pixels.

Keywords: Opium poppy field, EO-1 Hyperion, Hyperspectral data, Target detection, MTMF, Afghanistan

3.1 Introduction

3.1.1 Background

Drug abuse causes a serious societal problem in the word. Monitoring this problem starts with estimating how much drugs are produced. A principal indicator for the production size is the area under cultivation. However, it is usually challenging to investigate where opium poppy fields are through intensive field surveys.

Satellite images have wide spatial coverage and high temporal repeatability. With the recent surge in the availability of spectral imaging sensors, remote sensing presents a great potential to map vegetation and detect invasive plants (Xie et al., 2008; Huang and Asner, 2009). However, it is challenging to detect opium poppy fields from remote sensing images because training samples are usually extremely difficult to obtain

through field surveys. In general, opium poppy is planted in the regions or countries where bad transportation conditions and insecure environments exist. In particular, it is often unfeasible to conduct frequent and accurate field surveys in Afghanistan, the primary opium producer in the world, in which the potential production of opium represented 88% of global production in 2009 (UNODC, 2011).

The objective of this paper was to develop a practical and economical way to detect poppy fields from satellite images in Afghanistan. To make it suitable for the specific conditions in opium poppy producing regions in Afghanistan, the detection method should be unsupervised (i.e., not require training samples), and computationally efficient so that it can work well for detection in a huge area timely.

3.1.2 Previous Work

3.1.2.1 Work of Other Researchers

A comprehensive literature review by the authors found that only high resolution satellite multispectral images ($\leq$ 1 m), as well as the hyperspectral data collected by a handheld spectrometer in a laboratory experiment or in field surveys, have been used to differentiate poppy from other crops. When high spatial resolution multispectral imagery was used to detect opium poppy fields, visual interpretation was the main method. The United Nations Office on Drugs and Crime (UNODC) visually interpreted high resolution pan-sharpened images, like IKONOS, WorldView, QuickBird, GeoEye, etc., to identify opium poppy fields. Before the visual interpretation, medium resolution satellite imagery like Landsat 7 TM/ETM+ images (30 m) and Disaster Monitoring Constellation (DMC) satellite images (32m) were used to delineate the agricultural fields

(UNODC, 2009). UNODC often used a pair of high resolution images like IKONOS that were acquired at two stages, namely the pre-harvest (flowering or capsule) stage and the post-harvest (post-lancing) stage. Thus, the interpretation based on first-dated images was improved by comparing with second-dated images. However, the use of a pair of images is not suitable for poppy eradication before harvest. Besides UNODC, Taylor et al. (2010) and Tian et al. (2011) also interpreted high resolution satellite multispectral images (e.g., IKONOS, QuickBird) to map poppy in Afghanistan and Myanmar, respectively. Both of them used the visual interpretation method, but they did not mention if they used any image fusion method to enhance the spatial resolution of the images used.

Unfortunately, it is very costly to use high spatial resolution imagery for poppy field detection in a large region. It is not affordable in developing countries without foreign financial aid. In contrast, the multispectral images with medium spatial resolution, like 30 m Landsat images, are much less expensive. However, it is difficult to find an individual plant species in such images (He et al., 2011) because of the limited spectral bands which are not enough to discriminate similar spectral signatures shared by different vegetation species (Miao et al., 2011).

A potential alternative may be the hyperspectral data acquired by EO-1 Hyperion, the only spaceborne hyperspectral sensor in operation currently. Hyperion imagery is free of charge. Its spatial resolution is 30 m × 30 m, which is coarse relatively to poppy fields (about 15 m × 15 m or less to 100 m × 100 m) in Afghanistan. However, it has hundreds of narrow bands to represent the detailed spectral signatures of plants, which

may increase the detection capability of small targets at sub-pixel levels by conducting spectral unmixing.

Until now, there is little evidence that opium fields have been identified from any satellite or aerial hyperspectral images. Only a limited number of studies attempted to identify opium poppy using hyperspectral data collected by a handheld spectrometer in a laboratory experiment (e.g., Lowe, 2010) or field spectral surveys (e.g., Jia et al., 2011; Nakazawa et al., 2012). It is unclear if opium fields can be identified from EO-1 Hyperion images directly. Discriminating poppy from other crops using satellite images is much more complex and difficult than using hyperspectral data collected in laboratory experiments or field spectral surveys. Moreover, the spectral mixture of Hyperion images caused by the coarse spatial resolution (30 m) further increases the difficulty of poppy field detection dramatically.

3.1.2.2 Work of Wang et al. (2013)

To detect poppy fields from EO-1 Hyperion imagery in Afghanistan, Wang et al. (2013) have proposed an unsupervised multiple endmember spectral mixture analysis (MESMA)-based method. This method first identified pure pixels or endmembers (see Appendix I) of main vegetation components and non-vegetation component based on the image itself. No training samples were involved. Then, it used the MESMA, the most widely used spectral mixture analysis (SMA) method (Somers et al., 2011) to conduct spectral umixing to detect the poppy pixels. Different from the traditional unsupervised methods like K-mean and Iterative Self-Organizing Data Analysis Technique Algorithm

(ISODATA), this MESMA-based methodology did not require the parameter of class number that was often unavailable in Afghanistan.

Nevertheless, the MESMA is computationally expensive. The MESMA accounts for endmember variability by iteratively computing linear models using different sets of endmember combinations for each individual pixel. To reduce computation amount, various techniques have been proposed to identify optimal endmembers to reduce the number of endmembers of each component (e.g., Roberts et al., 1993, 1998; Roberts et al., 2003; Dennison and Roberts, 2003; Dennison et al., 2004; Clark, 2005). However, such optimization increases the subjectivity of endmember selection. More importantly, the MESMA works on over a hundred spectral bands of hyperspectral data, so it is not computationally efficient for the detection of poppy fields in a huge area.

The study presented here built upon the MESMA-based method, focusing on increasing the computationally efficient by replace the MESMA with the Mixture Tuned Matched Filtering (MTMF) in the methodology. The MTMF developed by Boardman (1998) is another popular SMA approach. It works faster because it just works on the first several Minimum Noise Fraction (MNF) bands.

3.2 Study Area and Materials

3.2.1 Study Area

A region near Laskar Gah, the capital of the Helmand Province, Afghanistan (Figure 3.1) was chosen as the study area in this study. The main source of irrigation

water for agriculture in this arid area is the Helmand River, the longest river in Afghanistan that flows through the center of the province (Harris, 2012).

In Helmand, opium poppy is planted in fall, with flowers appearing in late March or early April (Owens and Clifton, 1972; Sader, 1991). Flowering lasts two to three weeks, and then the capsule remaining is cut after the fall of the leaves to allow the latex to flow from it. The harvest extends from approximately mid-April to early May, usually ending two or three weeks before the wheat harvest begins. Within Afghanistan, the opium cultivation area in Helmand, the dominant opium cultivating province, was 63,307 ha, as 48% of the total opium cultivation area of the country in 2011; this province alone produced 52% of all Afghan opium in 2011 (UNODC, 2011). Meanwhile, Helmand was one of the most insecure provinces in this country, so any field monitoring was quite dangerous.

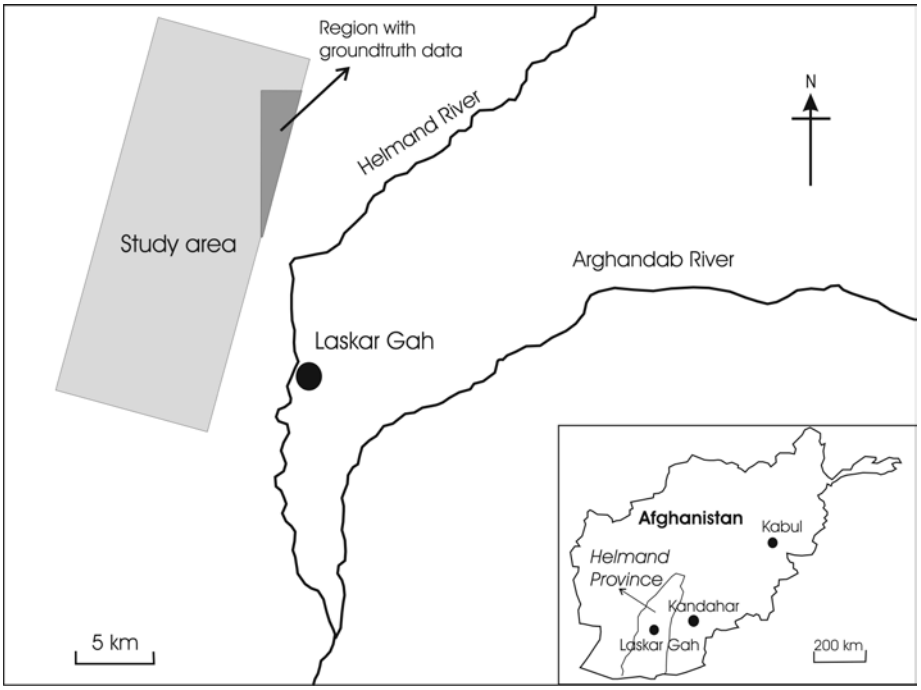

Figure 3.1 Study area

3.2.2 Materials

The interpretation files of opium fields that were provided by the UNODC were employed as surrogate groundtruth data to assess poppy field detection accuracies in this study. The interpretations, as part of "Opium Poppy Survey 2009" conducted by UNODC and Ministry of Counter Narcotics of Afghanistan, were based on an IKONOS image acquired on April 11, before harvest season, in 2009.

An EO-1 Hyperion hyperspectral image over the study area acquired on March 11th, 2009, a pre-harvest date, was applied in this study. The image was at level L1R processing, meaning that it was radiometrically but not geometrically corrected. In addition, a Landsat ETM+ image acquired on April 23, 2009 was applied to geometrically correct the Hyperion image.

3.3 Methodology

3.3.1 Hyperion Data Pre-processing

This study proposed an unsupervised MTMF-based method to detect poppy fields. This method consisted of four stages, i.e., Hyperion data pre-processing, endmember determination of main vegetation components, poppy pixel determination and detection accuracy assessment. The main difference from the MESMA-based method (Wang et al., 2013) was how to determine poppy pixels in the third stage. Another difference was that the MTMF-based method did not need to determine the endmembers of non-vegetation component.

Among the 242 spectral bands of Hyperion data, the bands that were intentionally not illuminated, correspond to areas of low sensitivity of the spectrometer materials, or too noisy due to atmospheric water vapor absorption were removed. The same subset of 121 selected bands (bands 8-56, 79-119, 135-164, and 195 within 426.8-2102.9 nm) were used in both of this study and Wang et al. (2013).

After band selection, the digital numbers (DN) of each pixel were converted into land surface reflectance through bad line fixing, vertical stripe removal, smile effect correction, atmospheric correction and geometric correction step by step. The bad lines were fixed by replacing their DN values with the average DN values of their immediate left and right neighboring pixels (Han et al., 2002). Vertical stripes were removed using the local destriping method (Datt et al., 2003). Smile effects were corrected using the procedure of "Cross-Track Illumination Correction" (Jupp et al., 2003) in the ENVI software (ITT Visual Information Solutions, Boulder, CO, USA). The correction of smile effect was assessed by checking if the first eigenvalue image after MNF transform displayed a brightness gradient or not (Green et al., 1988; Goodenough et al., 2003). Atmospheric effects were corrected by the Fast Line-of-sight Atmospheric Analysis of Spectral Hypercubes (FLAASH) module implemented in the ENVI. Then, geometric correction was conducted using the georeferencing tool in ArcMap (ESRI Inc., Redlands, California) by collecting 16 ground control points (GCPs) in reference to the Landsat 7 ETM+ imagery acquired on April 23, 2009 over the study area. An overall root mean square error (RMSE) of 7.06 m was achieved.

3.3.2 Endmember Determination of Main Vegetation Components

This study only considered the pixels with positive Normalized Difference Vegetation Index (NDVI) values that were computed from Band 31 (660.85 nm) and Band 44 (793.13 nm). MNF transform was applied to the spectral data to remove noises and reduce dimensionality of the hyperspectral image using the ENVI software. Then, Pixel Purity Index (PPI) values were calculated using the first six MNF bands with the highest eigenvalues. Only those pixels with PPI values not less than a preset PPI threshold were used to determine the vegetation endmembers, or spectrally pure vegetation pixels. Further, the pixels whose NDVI values were less than 0.2 were removed (Tsai et al., 2007; Noujdina and Ustin, 2008) because the MTMF-based method did not need to consider the non-vegetation pixels. This was different from the MESMA-based method. Then, the pixels whose red region reflectance was not less than green region reflectance were filtered out because they were not pure vegetation pixels considering the high absorption of chlorophyll at red region. The remaining pixels were seen as pure vegetation pixels, and they were displayed in the n-Dimensional Visualizer in the ENVI to determine endmembers of main vegetation components (e.g., poppy and wheat).

Wang et al. (2013) used 2000 as a PPI threshold. To investigate the effects of PPI threshold on the final poppy detection, this study used 2000 and 1500 as PPI thresholds, respectively. Using higher PPI threshold can find the "purer" endmembers, and meanwhile less endmembers can be selected. Regardless, using either 2000 or 1500 as the PPI threshold, the pure vegetation pixels formed two distinct vegetation clusters representing two kinds of vegetations in the n-Dimensional Visualizer in ENVI (Figure

3.2). The two main crops were poppy and wheat at the season in the study area in 2009, and poppy had lower NDVI value than wheat (UNDOC, 2009; Lowe, 2010). The averaged endmember of the pixels in the bottom-right cluster had a respective NDVI value of 0.77 or 0.76 when 2000 (Figure 3.2(a)) and 1500 (Figure 3.2(b)) were used as a PPI threshold, respectively, while the averaged endmember of the pixels in the top-left cluster had NDVI value of 0.85 in either Figure 3.2(a) or Figure 3.2(b). Hence, the bottom-right cluster was poppy and the top-left cluster was wheat. In total, 10 and 16 poppy endmembers and 21 and 38 wheat endmembers were selected when 2000 and 1500 were used as a PPI threshold, respectively.

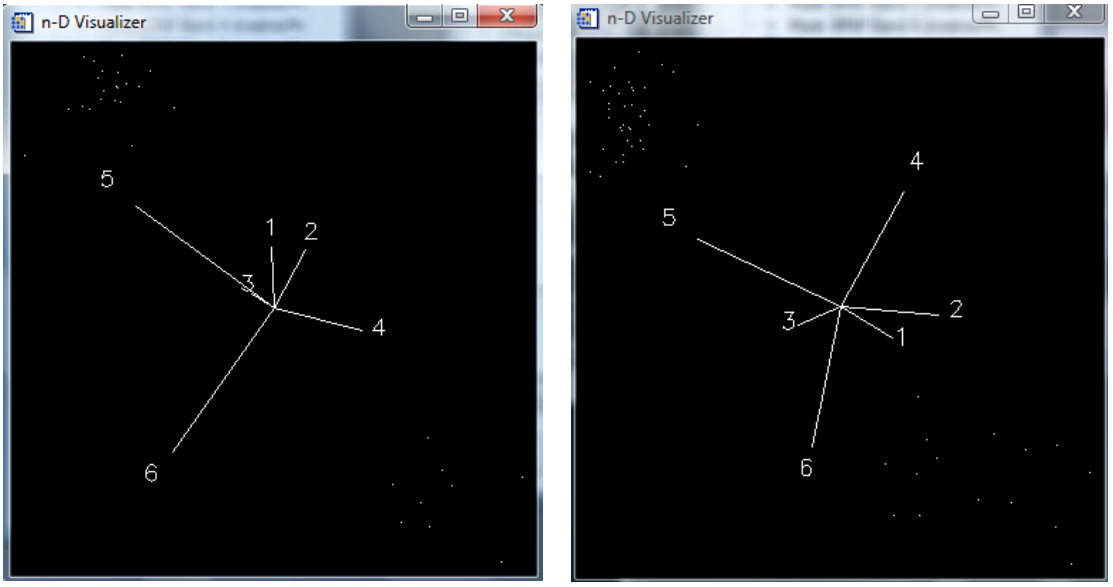

(a) (b)

Figure 3.2 The pure vegetation pixels formed two distinct vegetation clusters in the n-Dimensional Visualizer in ENVI, no matter either 2000 (a) or 1500 (b) was used as a PPI threshold. The numbers in the subfigures referred to MNF band numbers.

3.3.3 Poppy Pixel Determination

After the endmembers of poppy and wheat were determined, MNF-transformed spectral libraries for each endmember of each component were built by using the ENVI software. Meanwhile, an averaged MNF-transformed spectral library was also built for each component. This facilitated the comparison of effects of using multiple endmembers against that of using an averaged endmember on the poppy pixel detection accuracies.

To determine poppy pixels from the Hyperion image, the MTMF model of the ENVI was used to conduct spectral unmixing (Figure 3.3). The MTMF determined pixels in which the target endmember signal was statistically distinct from the average background pixels. It was run on the MNF-transformed Hyperion image using the component of poppy and that of wheat as target, respectively.

MTMF output two sets of images, i.e., matched filtering (MF) score image and Infeasibility image. Then, three thresholds or filters were used to eliminate the background pixels from further consideration: (1) MF > MF threshold, (2) Infeasibility < Infeasibility threshold, and (3) NDVI $\geq$ 0.2. In general, the pixels with a NDVI value less than 0.2 are non-vegetation (Tsai et al., 2007; Noujdina and Ustin, 2008). The remaining pixels were determined as poppy pixels if their MF values of poppy were higher than their MF values of wheat.

In the MTMF-based method, two thresholds (i.e., infeasibility threshold and MF threshold) need to be preset. Various infeasibility thresholds have been used in previous studies. For example, the threshold of 6 was used in Williams and Hunt (2002) and

Hassan and Hashim (2011) while the threshold of 15 was used in Mundt et al. (2005) to discriminate plant species. This study assessed three different infeasibility thresholds (i.e., 3, 4 and 6), respectively. As only very few pixels had higher infeasibility scores in the image, no thresholds higher than 6 were assessed. In addition, although the SMA approach of MTMF sees the pixels with zero or negative MF scores as background in existing literature, this study assessed the negative MF thresholds as well.

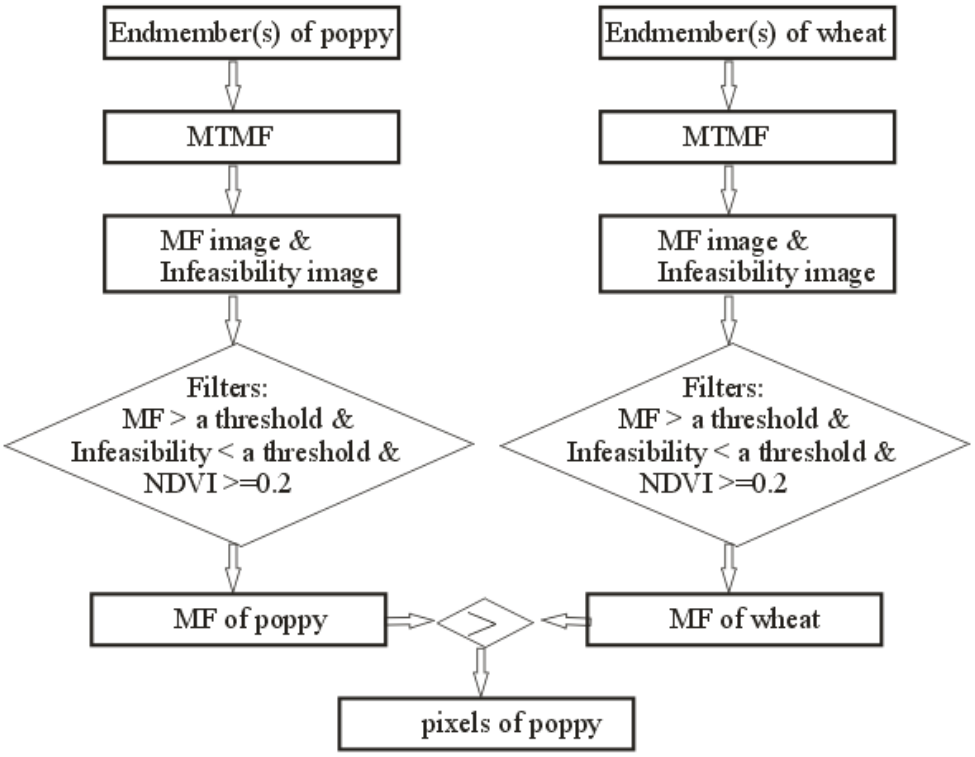

Figure 3.3 Workflow of poppy pixel determination in the MTMF-based methodology. The same set of thresholds was used for poppy and wheat.

3.3.4 Detection Accuracy Assessment

The retrieved poppy field distribution map had two classes, i.e., poppy pixels and non-poppy pixels. This distribution map was compared against the surrogate groundtruth data provided by UNODC pixel by pixel to calculate producer's, user's and overall accuracies as well as kappa coefficient for accuracy assessment.

3.4. Results

3.4.1 Effects of Involving More Endmembers in Each Component

In comparison to the use of the PPI threshold of 2000, more endmembers were selected for both of the components of poppy and wheat, respectively when a lower PPI threshold of 1500 was used. The resultant detection accuracies showed that involving more endmembers did not change the accuracies significantly (Table 3.1).

Table 3.1 Comparison of poppy field detection accuracies when different PPI thresholds, the same MF threshold (MF>0) and the same infeasibility threshold (Infeasibility<6) were used. Here, “multiple” refers that multiple endmembers were used, while “average” refers that an averaged endmember was used.

PPI	Endmember number	Accuracies			
		Producer's (%)	User's (%)	Overall (%)	kappa
≥2000	multiple	55	75	75	0.45
	average	49	75	74	0.41
≥1500	multiple	54	75	75	0.45
	average	49	75	74	0.42

3.4.2 Effects of Using Different Infeasibility Thresholds

Table 3.2 showed the effects of using different infeasibility thresholds on the classification accuracies. The threshold of "MF>0" was used in this experiment because it is a common knowledge in the SMA approach of MTMF. It was found that, whether only an averaged endmember was used or multiple endmembers were used, all accuracies, especially producer's accuracy, increased with increasing infeasibility thresholds. Since the infeasibility score describes in terms of noise standard deviations how likely it is that each pixel is a mixture of the known target and the background materials (Boardman and Kruse, 2011), it is expected that increasing the infeasibility threshold would reduce user's accuracy. However, user's accuracy increased with increasing infeasibility threshold in this study. This likely suggests that it is not necessarily correct that a lower infeasibility threshold leads to higher user's accuracy when general infeasibility scores are relatively low within an image.

In addition, producer' accuracies of 42%-49%, user's accuracies of 73%-75%, overall accuracies of 72%-74% and kappa coefficients of 0.36-0.41 were achieved when only an averaged endmember was considered (Table 3.2). In contrast, producer's accuracies of 50%-55%, user's accuracies of 74%-75%, overall accuracies of 74%-75% and kappa of 0.42-0.45 were achieved when multiple endmembers were considered. Therefore, in comparison to using an averaged endmember, using multiple endmembers increased producer's accuracy, overall accuracy and kappa significantly while user's accuracy did not show significant change, no matter which infeasibility threshold was used.

Table 3.2 Comparison of poppy field detection accuracies when the same PPI threshold (PPI≥2000), the same MF threshold (MF>0) but different infeasibility thresholds were used.

Infeasibility threshold	Accuracies	Using multiple endmembers	Using an averaged endmember
<6	Producer's	55	49
	User's	75	75
	Overall	75	74
	kappa	0.45	0.41
<4	Producer's	54	48
	User's	75	75
	Overall	75	74
	kappa	0.45	0.40
<3	Producer's	50	42
	User's	74	73
	Overall	74	72
	kappa	0.42	0.36

3.4.3 Effects of Using Various MF Thresholds

Four different values, i.e., -0.2, -0.1, 0 and 0.1 were used as a MF threshold, respectively to assess their effects on detection accuracies. It was found that MF thresholds had relatively smaller effects on user's accuracy and overall accuracy; user's

accuracies varied between 71% and 77%, and overall accuracies varied between 69% and 76% (Figure 3.4). However, producer's accuracy and kappa coefficient decreased significantly with increasing MF threshold from -0.2 to 0.1. In particular, when the MF score of 0.1 was used as a threshold, user's accuracies increased but all other accuracies decreased significantly. This is reasonable because using a higher MF threshold meant only the purer poppy pixels were included while those less pure poppy pixels were filtered out though they were also poppy pixels.

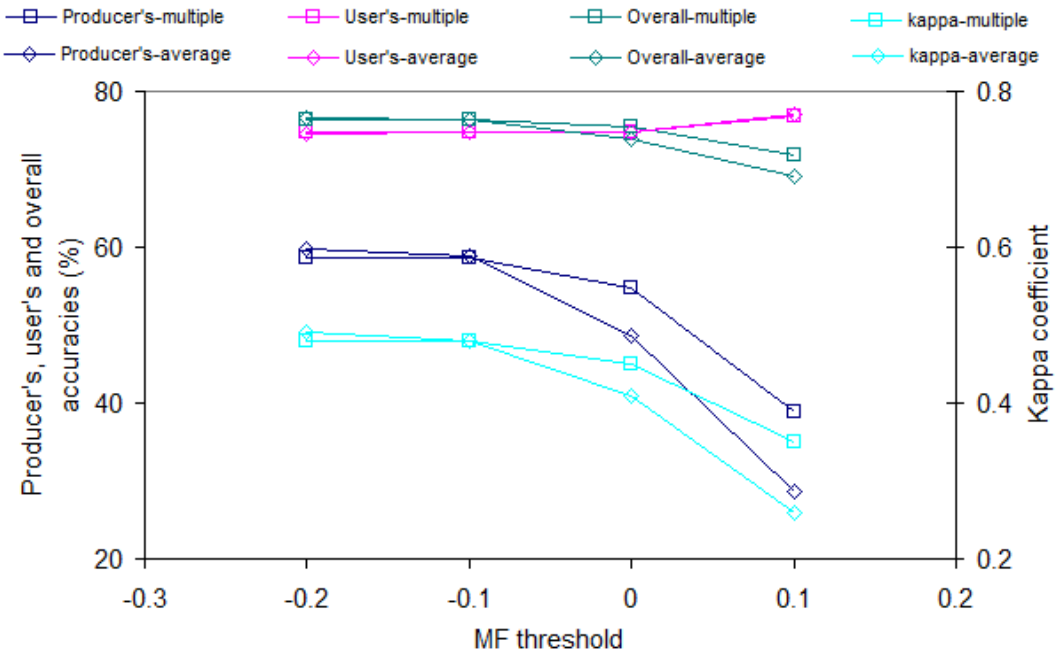

Figure 3.4 Comparison of poppy field detection accuracies when the same PPI threshold (PPI≥2000), the same infeasibility threshold (Infeasibility<6) but different MF thresholds were used. The "multiple" refers that multiple endmembers were used, while "average" refers that an averaged endmember was used.

The variations of all accuracies with increasing MF threshold were smaller when multiple endmembers rather than an averaged endmember were used, especially for

producer’s accuracy and kappa. In addition, using multiple endmembers generally could achieve higher detection accuracies than only using an averaged endmember, but the producer’s accuracy was an exception when negative MF score thresholds were used.

In addition, as shown in Figure 3.4, producer's accuracies were much lower than user’s accuracies and overall accuracies. Meanwhile, producer’s accuracies decreased with increasing MF thresholds. Therefore, it seemed that using MF score of -0.2 as a threshold could achieve the highest accuracies of poppy pixel detection.

3.4.4 Poppy Distribution Map

As shown above, the highest detection accuracies were achieved when the MF threshold of -0.2 and the infeasibility threshold of 6 were used. This produced producer's, user’s and overall accuracies of 61%, 73% and 76%, and the resultant kappa coefficient was 0.48, representing moderate agreement between retrieved poppy distribution and groundtruth data. These accuracies were similar to those achieved using the MESMA-based method in Wang et al. (2013), but this MTMF-based method worked over 10 times faster.

The derived distribution of poppy pixels was shown in Figure 3.5(a). Surrogate groundtruth data of poppy (Figure 3.5(c1)) were available for the subarea within the box “b1”, which seemed similar to its counterpart (Figure 3.5(b1)) retrieved in this study. This was also supported by the comparison between them for an enlarged part (i.e., Figure 3.5(b2) with Figure 3.5(c2)).

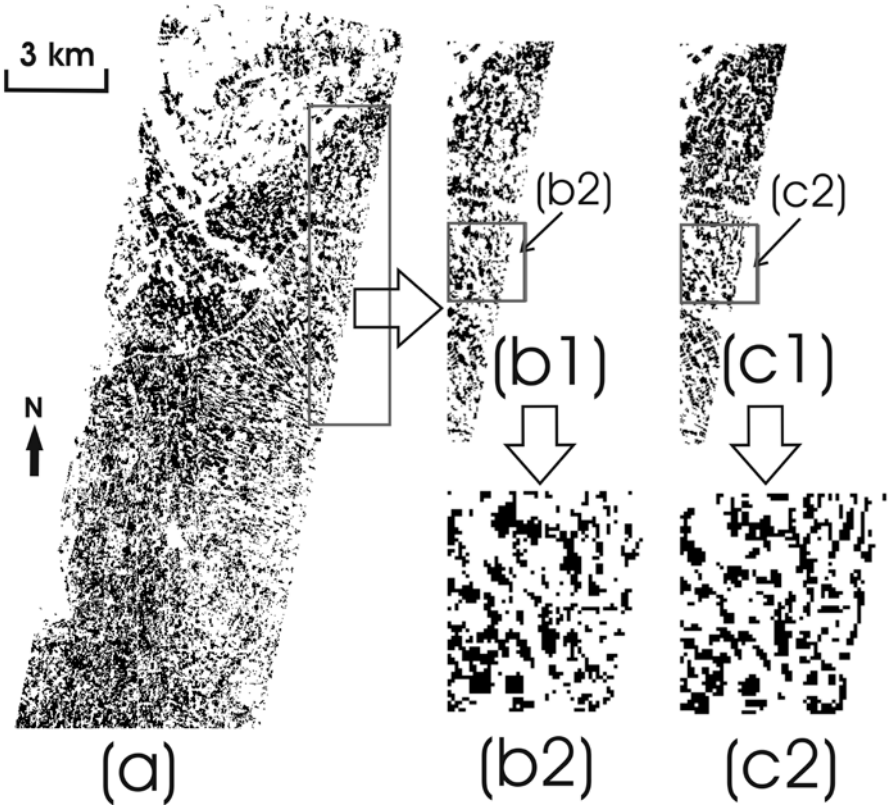

Figure 3.5 Poppy distribution map (a) retrieved from an EO-1 Hyperion image over the study area acquired on March 11, 2009. Groundtruth map of poppy (c1, and its subset c2) only covered the area within the box "b1" was compared with counterpart (b1, and its subset b2).

3.5 Discussion and Conclusions

In the MTMF-based method, two thresholds (i.e., infeasibility threshold and MF threshold) need to be preset. This study assessed the effects of using different thresholds on the detection accuracies of poppy fields. Three different infeasibility thresholds (i.e., 3, 4 and 6) were assessed, respectively. In general, using 4 as a threshold could increase all accuracies compared with using 3 as a threshold while using 4 or 6 as thresholds led

to similar accuracies. The reason may be that there were only few pixels with infeasibility scores greater than 4. As shown in Figure 3.6, most pixels had infeasibility scores smaller than 3 for both poppy and wheat. Only 14.7% and 13.9% of pixels had infeasibility scores that were greater than or equal to 3 for poppy and wheat, respectively. Such percentages decreased significantly to only 3.2% and 2.8% at the infeasibility score of 4. Further, only 0.3% and 0.4% of pixels had infeasibility scores that were greater than or equal to 6 for poppy and wheat, respectively. This also explained why the infeasibility thresholds greater than 6 were not analyzed in this study.

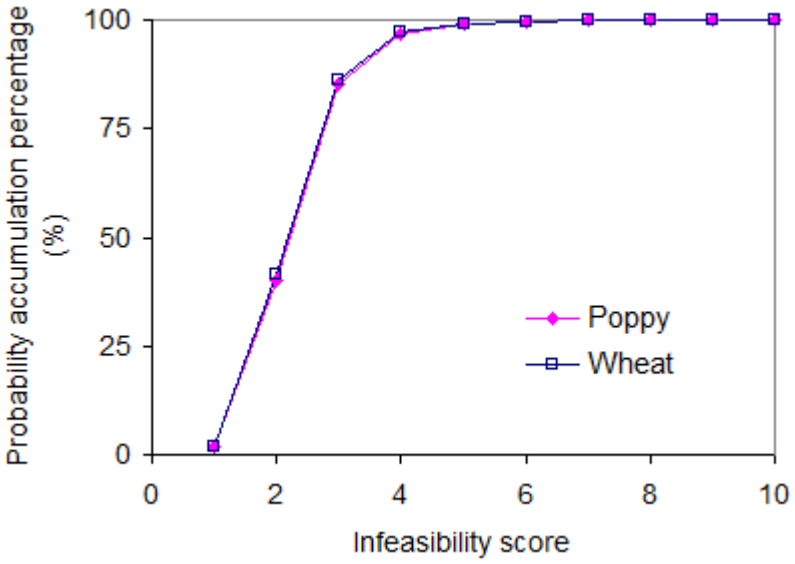

Figure 3.6 Probability accumulation percentage verse infeasibility score

As for the MF threshold, to the authors' knowledge, only the MF scores of 0 or higher values were used as a threshold in existing literature. This is because the SMA approach of MTMF projects the mean of the background data to zero, i.e., half of the background will have negative values (Robichaud et al., 2007). However, the present

study found that a large number of the pixels with zero or negative MF scores were also poppy pixels. Ignoring these pixels reduced producer's accuracy and kappa coefficient markedly (Figure 3.4). The main reason should be the high spectral similarity between poppy and wheat. As the MTMF only sees one component as target, and it sees all others as background, such high spectral similarity made it quite difficult to determine the target of poppy from the background including wheat. Therefore, when the MTMF was run in a traditional way, i.e., the pixels with zero or negative MF scores were seen as background, the producer's accuracy and kappa coefficient were too low to detect poppy fields effectively.

Thus, the use of MF threshold of -0.2 and the infeasibility threshold of 6 was found to be able to produce the highest detection accuracies. The retrieved poppy field distribution map showed significant agreement with surrogate groundtruth data. The resultant producer's, user's, overall accuracies and kappa coefficient were 61%, 73%, 76% and 0.48, respectively. The number of derived poppy pixels covered 83% of the number of real poppy pixels. This was achieved under the circumstances that no training data were available and meanwhile only free EO-1 Hyperion imagery, the only spaceborne hyperspectral sensor, with 30-m coarse resolution and low SNR (Kruse et al., 2003) was available. Such circumstances were quite typical in the study area. Moreover, the Hyperion image acquisition date also hindered from achieving higher detection accuracies to some extent. In the study area, poppy flowers appeared in late March or early April (Sader, 1991). The used Hyperion image was acquired on March 11, before the flowering season due to the availability of Hyperion images. This increased the difficulty in detection of poppy fields because the optimum timing of imagery for the

discrimination of poppy from a range of other field crops was the flowering stage (Sader, 1991; Taylor et al., 2010; Jia et al., 2011).

In general, this study achieved similar accuracies of poppy field detection to Wang et al. (2013). However, the MTMF-based method worked over 10 times faster in this study. This is because the MTMF only needs to work on the first several MNF-transformed bands. In contrast, the MESMA-based approach has to work on over 100 individual spectral bands. Simple and fast method is critical to poppy field detection in a huge region like Afghanistan where opium poppy is widely planted.

In future research, the MTMF-based method will be applied to other regions in Afghanistan to check if the same set of thresholds are suitable for different environments. In addition, image fusion of Hyperion and ALI images will be conducted to improve the performance of the MTMF-based methodology on poppy field detection. Fusing Hyperion's 30m hyperspectral bands with ALI's 10m Panchromatic band can enhance Hyperion data's spatial resolution (Memarsadeghi et al., 2005; Capobianco et al., 2007; Pour and Hashim, 2013). Both Hyperion and ALI sensors are carried by the EO-1 platform. Having both Hyperion and ALI on the same platform reduces temporal effects on registration accuracy greatly.

Acknowledgements

This work was supported by the Canada Research Chairs Program. The authors thank the United Nations Office on Drugs and Crime (UNODC) for providing the interpretation files of opium fields. The views expressed in this paper are those of the author(s) and do not necessarily reflect the views of the United Nations.

References

Boardman, J.W. (1998). "Leveraging the high dimensionality of AVIRIS data for improved sub pixel target unmixing and rejection of false positives; Mixture Tuned Matched Filtering." *Summaries of the 7th JPL Airborne Earth Science Workshop* (Jet Propulsion Laboratory Publication), 1, pp. 53.

Boardman, J.W., and F.A. Kruse (2011) "Analysis of Imaging Spectrometer Data Using N-Dimensional Geometry and a Mixture-Tuned Matched Filtering Approach." *IEEE Transactions on Geoscience and Remote Sensing*, Vol. 49, No. 11, pp. 4138-4152.

Capobianco, L., A. Garzelli, L.A. Filippo Nencini, and S. Baronti (2007). "Spatial enhancement of Hyperion hyperspectral data through ALI panchromatic image." *IEEE International Geoscience and Remote Sensing Symposium (IEEE, 2007)*, 5158–5161.

Clark, M. (2005). "An assessment of Hyperspectral and Lidar Remote Sensing for the Monitoring of Tropical Rain Forest Trees." PhD dissertation, University of California, Santa Barbara, 319p.

Datt, B., T.R. McVicar, T.G. Van Niel, D.L.B. Jupp, and J.S. Pearlman (2003). "Preprocessing EO-1 Hyperion Hyperspectral Data to Support the Application of Agricultural Indexes." *IEEE Transactions on Geoscience and Remote Sensing*, Vol. 41, No. 2, pp. 1246-1259.

Dennison, P.E., and D.A. Roberts (2003). "Endmember Selection for Multiple Endmember Spectral Mixture Analysis using Endmember Average RSME." *Remote Sensing of Environment*, Vol. 87, pp. 123-135.

Dennison, P.E., K.Q. Halligan, and D.A. Roberts (2004). "A Comparison of Error Metrics and Constraints for Multiple Endmember Spectral Mixture Analysis and Spectral Angle Mapper." *Remote Sensing of Environment*. Vol. 93, pp. 359-367.

Goodenough, D.G., A. Dyk, K.O. Niemann, J.S. Pearlman, H. Chen, T. Han, M. Murdoch, and C. West (2003). "Processing Hyperion and ALI for forest classification," *IEEE Transactions on Geoscience and Remote Sensing*, Vol. 41, pp. 1321-1331.

Green, A.A., M. Berman, P. Switzer, and M.D. Craig (1988). "A transformation for ordering multispectral data in terms of image quality with implications for noise removal." *IEEE Transactions on Geoscience and Remote Sensing*, Vol. 26, pp. 65-74.

Han, T., D.G. Goodenough, A. Dyk, and J. Love (2002). "Detection and correction of abnormal pixels in Hyperion image." *IEEE International Geoscience and Remote Sensing Symposium*, Vol. III, Toronto, ON, Canada, 1327–1330.

Harris, W. (2012). "Agriculrural review of Helmand Afghanistan." [Online] June 10, 2013: http://www.fresnostate.edu/jcast/cab/documents/pdf/adapt/HELMAND.pdf.

Hassan, N., and M. Hashim (2011). "Decomposition of mixed pixels of ASTER satellite data for mapping Chengal (Neobalanocarpus heimiisp) tree." Paper presented at 2011 IEEE International Conference on Control System, Computing and Engineering, ICCSCE 2011, November 25, 2011 -November 27, 2011, Penang, Malaysia, IEEE Computer Society.

He, K.S., D. Rocchini, M. Neteler, and H. Nagendra (2011) "Benefits of hyperspectral remote sensing for tracking plant invasions." *Diversity and Distributions*, Vol. 17, pp. 381–392.

Huang, C., and G. Asner (2009). "Applications of remote sensing to alien invasive plant studies." *Sensors*, Vol. 9, pp. 4869-4889.

Jia, K., B. Wu, Y. Tian, Q. Li, and X. Du (2011). "Spectral discrimination of opium poppy using field spectrometry." *IEEE Transactions on Geoscience and Remote Sensing*, Vol. 49, No. 9, pp. 3414-3422.

Jupp, D.L.B., B. Datt, T.R. McVicar, T.G. Van Niel, J.S. Pearlman, J.L. Lovell, and E.A. King (2003). "Improving the analysis of Hyperion red-edge index from an agricultural area." *Proceedings of SPIE*, Vol. 4898, pp. 1-15.

Kruse, F., J. Boardman, and J. Huntington (2003). "Comparison of airborne hyperspectral data and EO-1 Hyperion for mineral mapping." *IEEE Transactions on Geoscience and Remote Sensing*, Vol. 41, pp. 1388-1400.

Lowe, A. (2010). "Remote Sensing based Monitoring of Opium Cultivations in Afghanistan." Master dissertation, University of Bonn, 106 p.

Memarsadeghi, N., J. Le Moigne, D.M. Mount, and J. Morisette (2005). "A new approach to image fusion based on cokriging." *Proceedings of The Eight International Conference on Information Fusion (Fusion 2005)*, Philadelphia, PA, 2005, 1, 622-629.

Miao, X., R. Patil, J.S. Heaton, and R.C. Tracy (2011). "Detection and classification of invasive saltcedar through high spatial resolution airborne hyperspectral imagery." *International Journal of Remote Sensing*, Vol. 32, No. 8, pp. 2131-2150.

Mundt, J., N.F. Glenn, K.T. Weber, T.S. Prather, L.W. Lass, and J. Pettingill (2005). "Discrimination of hoary cress and determination of its detection limits via hyperspectral image processing and accuracy assessment techniques." *Remote Sensing of Environment*, Vol. 96, pp. 509−517.

Nakazawa, A., J.H. Kim, T. Mitani, S. Odagawa, T. Takeda, C. Kobayashi, and O. Kashimura (2012). "A study on detecting the poppy field using hyperspectral remote sensing techniques." 2012 IEEE International Geoscience and Remote Sensing Symposium (IGARSS), 22-27 July 2012, Munich.Page(s): 4829 - 4832 (DOI: 10.1109/IGARSS.2012.6352532).

Noujdina, N.V., and S.L. Ustin (2008). "Mapping Downy Brome (Bromus tectorum) using multidate AVIRIS data." *Weed Science*, Vol. 56, pp. 173–179.

Owens, G.P., and J.H. Clifton (1972). "Poppies in Afghanistan." USAID - Kabul, Afghanistan, 34 p.

Pour, A.B., and M. Hashim (2013). "Fusing ASTER, ALI and Hyperion data for enhanced mineral mapping." *International Journal of Image and Data Fusion*, Vol. 4, No. 2, pp. 126-145.

Roberts, D.A., J.B. Adams, and M.O. Smith (1993). "Discriminating Green Vegetation, Non-Photosynthetic Vegetation and Soils in AVIRIS Data." *Remote Sensing of Environment*, Vol. 44, pp. 255-269.

Roberts, D.A., P.E. Dennison, M. Gardner, Y. Hetzel, S.L. Ustin, and C. Lee (2003). "Evaluation of the Potential of Hyperion for Fire Danger Assessment by Comparison to the Airborne Visible/Infrared Imaging Spectrometer." *IEEE Transactions on Geoscience and Remote Sensing*, Vol. 41, No. 6, pp. 1297-1310.

Roberts, D.A., M. Gardner, R. Church, S. Ustin, G. Scheer, and R.O. Green (1998). "Mapping Chaparral in the Santa Monica Mountains using Multiple Endmember Spectral Mixture Models." *Remote Sensing of Environment*, Vol. 65, pp. 267−279.

Robichaud, P.R., S.A. Lewis, D.Y.M. Laes, A.T. Hudak, R.F. Kokaly, and J.A. Zamudio (2007) "Postfire soil burn severity mapping with hyperspectral image unmixing." *Remote Sensing of Environment*, Vol. 108, pp. 467-480.

Sader, S.A. (1991). "Remote Sensing of Narcotic Crops with special reference to techniques for detection and monitoring of poppy production in Afghanistan." [Online] June 9, 2013: http://pdf.usaid.gov/pdf_docs/PNABT431.pdf.

Somers, B., G.P. Asner, T. Laurent, and P. Coppin (2011). "Endmember variability in Spectral Mixture Analysis: A review." *Remote Sensing of Environment*, Vol. 115, No. 7, pp. 1603-1616.

Taylor, J.C., T.W. Waine, G.R. Juniper, D.M. Simms, and T.R. Brewer (2010). "Survey and monitoring of opium poppy and wheat in Afghanistan: 2003-2009." *Remote Sensing Letters*, Vol. 1, No. 3, pp. 179–185.

Tian Y.C., B.F. Wu, L. Zhang, Q.Z. Li, K. Jia, and M.P. Wen (2011). "Opium poppy monitoring with remote sensing in North Myanmar." *International Journal of Drug Policy*, Vol. 22, pp. 278–284.

Tsai, F., E.-K. Lin, and K. Yoshino (2007). "Spectrally segmented Principal Component Analysis of hyperspectral imagery for mapping invasive plant species." *International Journal of Remote Sensing*, Vol. 28, pp. 1023–1039.

UNODC (2009). "Afghanistan Opium Survey 2009." [Online] October 16, 2012: http://www.unodc.org/documents/crop-monitoring/Afghanistan/Afgh-opiumsurvey2009_web.pdf.

UNODC (2011). "Afghanistan Opium Survey 2011." [Online] October 16, 2012: http://www.unodc.org/documents/crop-monitoring/Afghanistan/Afghanistan_opium_survey_2011_web.pdf.

Wang, J.J., Y. Zhang, and C. Bussink (2013). "Remote Sensing of Opium Poppy Fields Using EO-1 Hyperion Hyperspectral Data: an Example in Afghanistan." *Proceedings of the 2013 Canadian Institute of Geomatics Annual Conference and the 2013 International Conference on Earth Observation for Global Changes (EOGC'2013)*, 5-7 June 2013, Toronto, Ontario, Canada, pp. 106-110.

Williams, A.P., and E.R.Jr. Hunt (2002). "Estimation of leafy spurge cover from hyperspectral imagery using mixture tuned matched filtering." *Remote Sensing of Environment*, Vol. 82, pp. 446–456.

Xie, Y. (2008) "Remote sensing imagery in vegetation mapping: A review." *Journal of Plant Ecology*, Vol. 1, No. 1, pp. 9-23.

CHAPTER 4

AN UNSUPERVISED APPROACH TO DETECT OPIUM POPPY FIELDS IN BATI KOT, NANGARHAR, AFGHANISTAN, USING EO-1 HYPERION DATA

* This paper is co-authored by Wang, J.J. and Zhang, Y., and it will be submitted to *Remote Sensing (peer-reviewed Open Access journal)*.

Abstract

Detection of opium poppy fields is a big challenge in Afghanistan. In this insecure and developing country where the poppy is planted nationwide, a practical poppy field detection technique must be unsupervised, low-cost and computationally efficient. Wang et al. (2013b) have proposed an unsupervised Mixture Tuned Matched Filtering (MTMF)-based method to detect poppy fields from EO-1 Hyperion hyperspectral imagery that is free of charge but has a coarse spatial resolution. This method performed well in a study area located in the arid plateau in southwest Afghanistan. This study aimed to further test if this method could also detect poppy fields effectively in a different environment. The test employed a Hyperion image acquired in 2004, another year, and it did not use any training samples, too. It was found that the MTMF-based method also performed well in a new study area located in the Kabul River floodplain in mountainous East Afghanistan, another main environmental type in the country. Thus, the MTMF-based method may help better understand the temporal changes of poppy

cultivation during the past decade in Afghanistan from the archives of EO-1 Hyperion images in future research.

Keywords: Opium poppy field, EO-1 Hyperion, Hyperspectral data, Target detection, MTMF, Bati Kot, Afghanistan

4.1 Introduction

In the fight against drug abuse, one of main challenges is how to monitor illegal opium poppy fields timely. Field surveys are expensive and time-consuming for a huge region like Afghanistan, the dominant opium producer in the entire world (UNODC, 2009). Sometime, field surveys are unfeasible due to security reasons or transportation conditions in this country. This highlights the importance of satellite remote sensing application in poppy field detection.

In previous studies, satellite images have been used for opium poppy field detection (e,g., UNODC, 2009; Taylor et al., 2010; Tian et al., 2011). However, these studies heavily relied on expensive high spatial resolution (≤ 1m) multispectral images. For instance, United Nations Office on Drugs and Crime (UNODC) detected opium poppy fields by visually interpreting high-resolution images such as pan-sharpened IKONOS (UNODC, 2009). In contrast, moderate spatial resolution satellite imagery like Landsat 7 TM/ETM+ images (30 m) and Disaster Monitoring Constellation (DMC) images (32 m) were only used to delineate the agricultural fields before detecting opium poppy fields.

The high cost per area unit of high spatial resolution imagery makes the mapping of full coverage of the crop an expensive exercise in a huge area like Afghanistan where opium poppy is widely planted. Hence, Wang et al. (2013a, 2013b) have attempted to detect poppy fields from moderate spatial resolution (i.e., 30 m) EO-1 Hyperion hyperspectral imagery which is free of charge. Hyperion is the only spaceborne hyperspectral sensor currently in place and available. Although, to authors' knowledge, no satellite or aerial hyperspectral images have been used to detect opium poppy fields in other researchers' studies, the hundreds of narrow bands of hyperspectral data make it possible to detect subpixel size targets (Manolakis, 2002).

Wang et al. (2013a, 2013b) selected a study area located at central Helmand Province, Afghanistan. An unsupervised Multiple Endmember Spectral Mixture Analysis (MESMA)-based method and an unsupervised Mixture Tuned Matched Filtering (MTMF)-based one were proposed to detect poppy field from an EO-1 Hyperion image covering the study area. The two methods performed well under the circumstance that no training samples of poppy fields were available. This was important because it was extremely difficult to obtain training samples through field surveys in Afghanistan. Between the two methods that achieved similar detection accuracies, the MTMF-based one has much higher computational efficiency.

However, it was still unclear if the MTMF-based method could also detect poppy fields from a different EO-1 Hyperion image that was acquired in a different year and covered a different study area in the country. As the study area in Wang et al. (2013a, 2013b) was located in the arid plateau in southwest Afghanistan, this study focused on Nangarhar Province in mountainous east Afghanistan to test this MTMF-based method.

4.2 Study Area

Afghanistan has gradually become the largest opium producer in the entire world, providing 86% of global illicit opium supply in 2004 (UNODC, 2005). Within the country, the single largest opium producing province in 2004 was Nangarhar (23% of total), followed by Helmand (20%), Badakshan (18%) and Uruzgan (8%) (UNODC, 2004). In Nangarhar, opium poppy accounted for more than 76% of wheat cultivation (i.e., opium poppy was equivalent to 76% of the area under wheat cultivation) in 2004; in the villages surveyed, more than 80% of the families were involved in poppy cultivation (UNODC, 2004).

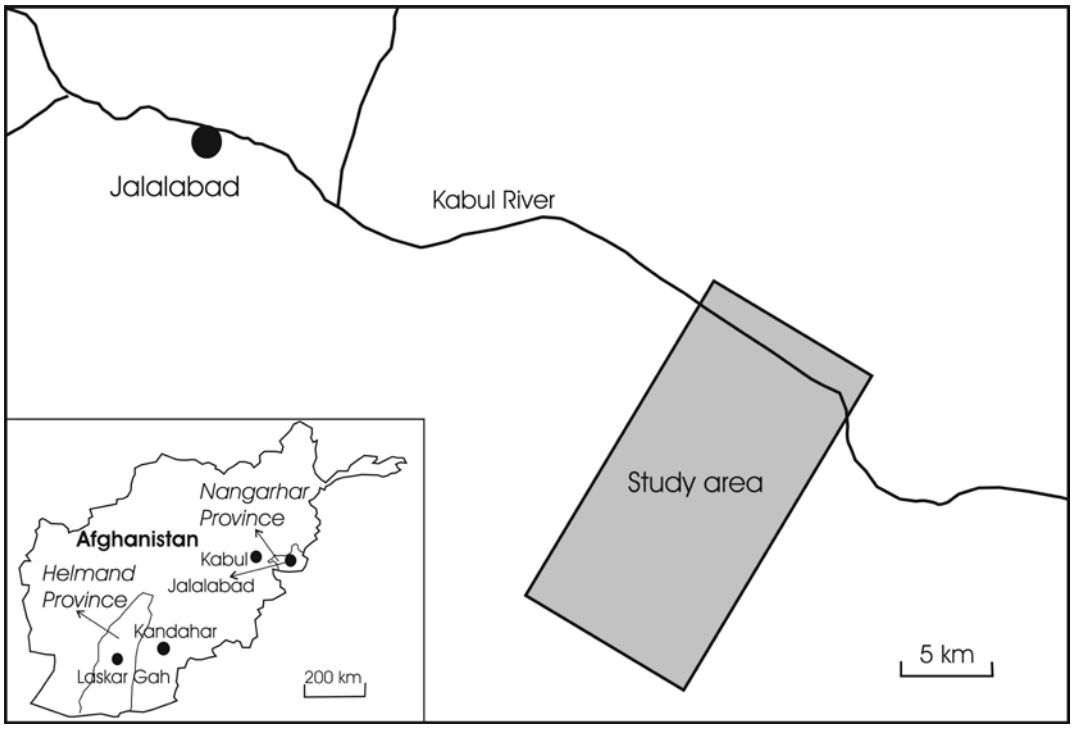

Figure 4.1 Study area of Bati Kot, Nangarhar, Afghanistan

Within Nangarhar, the largest opium producing province in 2004, half of the cultivation took place in just five districts (i.e., Rodat, Khogyani, Bati Kot, Kams and

Sherzad) (UNODC, 2004). Bati Kot, among the five districts, was selected as a study area (Figure 4.1). Bati Kot district is located east of Jalalabad, the capital of Nangarhar Province. It is on the Kabul River floodplain, consisting of largely agricultural land.

4.3 Data and Methodology

4.3.1 Data

An EO-1 Hyperion hyperspectral image over the study area acquired on March 21, 2004, a pre-harvest date, was employed in this study. The image was at level L1R processing, meaning that it was radiometrically but not geometrically corrected. To geometrically correct the Hyperion image, a Landsat ETM+ image acquired on April 20, 2004 was applied.

This study could not find any good quality groundtruth data of poppy field of the study area. However, there was a poppy field distribution map of Nangarhar Province printed in "Afghanistan Opium Survey 2004" (UNODC, 2004). Although the resolution of the map was too coarse to provide detailed information of poppy field distribution for the study area, it was used as groundtruth data as it was the only one available to this study.

The poppy fields shown in this map were identified using remote sensing technique by UNODC (2004). Their methodology of survey was based on a sampling approach which combined the analysis of satellite images and extensive field visits. For the sampled areas, highly costing high-resolution IKONOS satellite images were interpreted, aided by copious ground data including crop types, GPS coordinates and

photographs. To fully cover the whole of Nangarhar province, the largest opium producing province in 2004, less expensive 10 metre resolution SPOT-5 multi-spectral image pairs, for both pre- and post-harvest season, were used. UNDOC (2004) indicated that the overall results of the two surveys (SPOT-5 and IKONOS) proved to be very similar.

4.3.2 Methodology

This study applied the MTMF-based method proposed in Wang et al. (2013b) to detect poppy fields in the study area. This method consisted of four stages, i.e., data pre-processing, endmember (see Appendix I) determination of main vegetation components (i.e., main vegetation species), poppy pixel determination and detection accuracy assessment. The detailed procedures of Hyperion data pre-processing and endmember determination have been described in Wang et al. (2013a, 2013b). After removing the bands that were intentionally not illuminated, corresponded to areas of low sensitivity of the spectrometer materials, or were too noisy due to atmospheric water vapor absorption, the subset of 120 bands (i.e., Bands 8-56, 83-97, 101-114, 116-117, 133-164, 195-196, 203-206, 211-212 within 426.8-2274.4 nm) were applied in this study.

Then, bad line fixing, vertical stripe removal as well as smile effect correction were conducted step by step following Han et al. (2002), Datt et al. (2003) and Jupp et al. (2003), respectively before correcting atmospheric effects using the Fast Line-of-sight Atmospheric Analysis of Spectral Hypercubes (FLAASH) module implemented in the ENVI software (ITT Visual Information Solutions, Boulder, CO, USA). After atmospheric correction, geometric correction was conducted as the used Hyperion image

was at Level 1R (L1R). The atmospherically corrected image was projected to UTM 41N, datum WGS 84 first. Then, geometric correction was conducted on the Hyperion image using the ENVI by collecting 33 ground control points (GCPs) in reference to the Landsat 7 ETM+ imagery that was acquired on April 20, 2004 over the study area. An overall root mean square (RMS) error of 0.49 pixel was achieved.

To select endmembers of main vegetation components, Normalized Difference Vegetation Index (NDVI) values were first computed from Band 31 (660.85 nm) and Band 44 (793.13 nm) for each pixel. Only the pixels with NDVI values greater than 0 were used in further analysis. A Minimum Noise Fraction (MNF) transform was applied to remove noises and reduce dimensionality of the hyperspectral image. Then, Pixel Purity Index (PPI) values representing a pixel's purity and spectral extremity were calculated from the MNF transformed data. Only those pixels with PPI values not less than a preset PPI threshold of 1500 were used to determine the endmembers of each component. This study used the PPI threshold of 1500 because Wang et al. (2013b) found that using either 2000 or 1500 as the PPI threshold produced similar detection accuracies.

Among the remaining pixels, the pixels whose red region reflectance was not less than green region reflectance were filtered out because they were not pure vegetation pixels according to the high absorption of chlorophyll at red region. The other 207 pixels were input into the n-Dimensional Visualizer in the ENVI software for the clustering process, which clustered the 207 pixels into three distinct groups (Figure 4.2) representing three kinds of vegetations as shown in Figure 4.3. Component C was the tree component because of their dark red color in false color image as well as their lower

NDVI values (i.e., 0.57). Components A and B were poppy and wheat, respectively because the two main crops were poppy and wheat at the season in the study area in 2004 (UNODC, 2004). According to UNDOC (2009) and Lowe (2010), poppy had lower NDVI value than wheat. So, Component A whose NDVI value was 0.70 should be poppy and Component B whose NDVI value was 0.77 should be wheat. Moreover, the reflectance of Components A and B were similar to that of poppy and wheat retrieved in Wang et al. (2013a, 2013b). After endmember selection, averaged MNF-transformed spectral libraries were built for each component (i.e., poppy, wheat and tree) by using the ENVI.

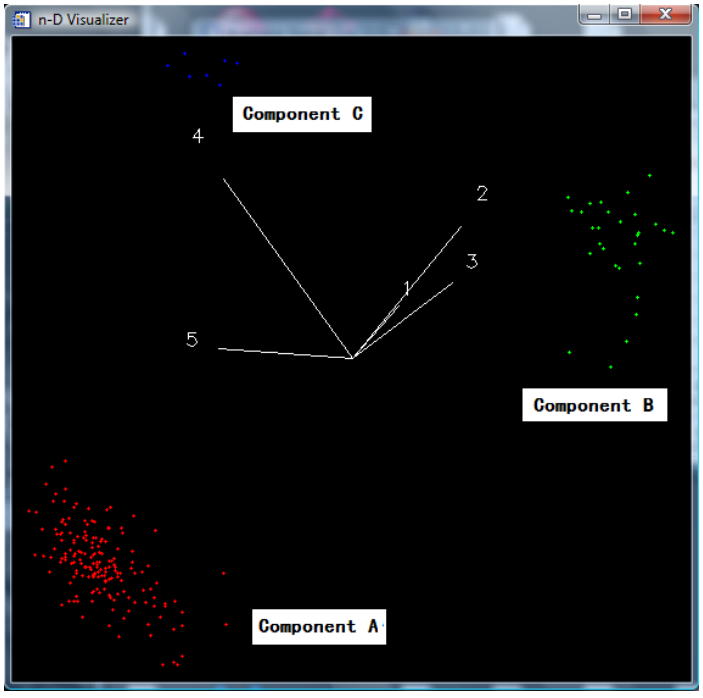

Figure 4.2 The 207 vegetation endmembers formed three distinct vegetation clusters, i.e., Components A (poppy), B (wheat) and C (tree) in the n-Dimensional Visualizer in the ENVI.

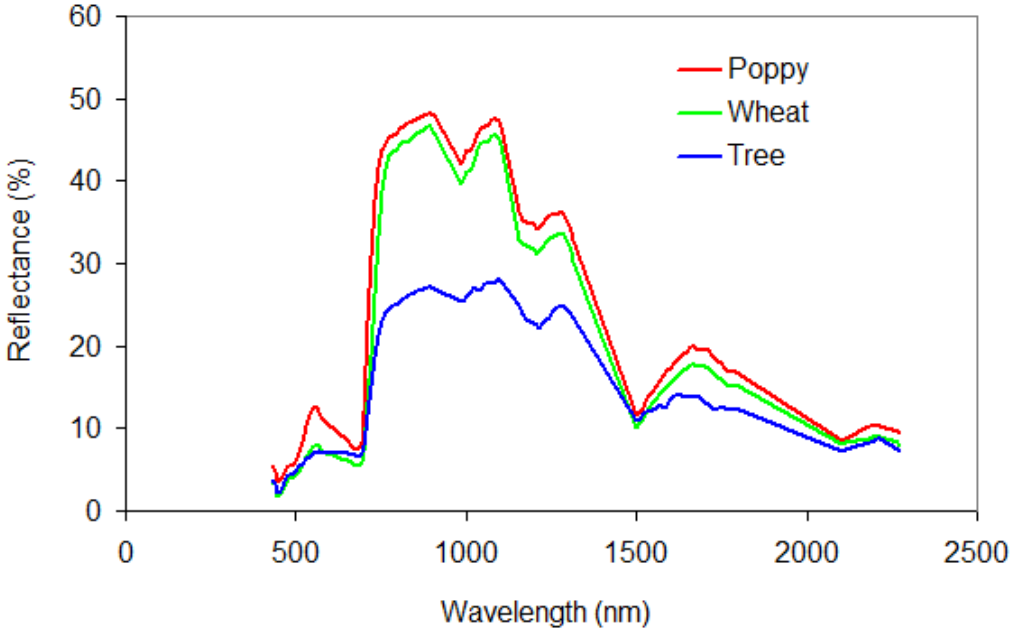

Figure 4.3 Spectral profile of averaged reflectance of endmembers in the three vegetation clusters, i.e., Components A (poppy), B (wheat) and C (tree), respectively.

The workflow of poppy pixel determination was shown in Figure 4.4. The MTMF determines pixels in which the target endmember signal is statistically distinct from the average background pixels. The MTMF was applied using the ENVI software. It was run on the MNF-transformed Hyperion image using each component of poppy, wheat and tree as target, respectively.

MTMF output two sets of images, i.e., MF score image and Infeasibility image. Then, three thresholds or filters that were found to be able to produce the highest detection accuracies in Wang et al. (2013b) were also used in this study: (1) MF > -0.2, (2) Infeasibility < 6, and (3) NDVI ≥ 0.2. The pixels with NDVI less than 0.2 are non-vegetation (Tsai et al., 2007; Noujdina and Ustin, 2008). The remaining pixels were

determined as poppy pixels if their MF scores of poppy were higher than their MF scores of wheat and of tree.

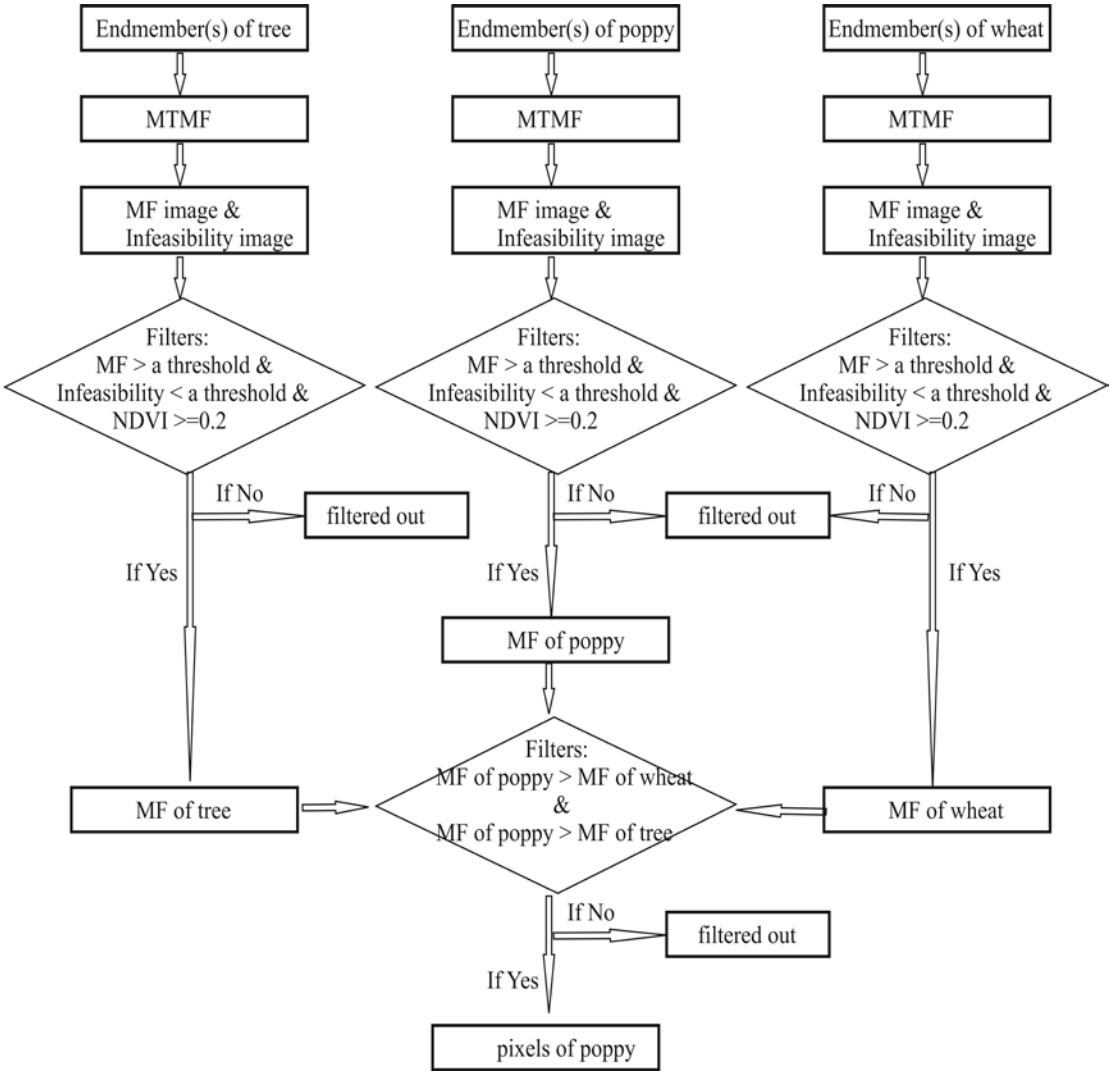

Figure 4.4 Methodology workflow of poppy field determination

4.4 Results

Poppy fields, as shown in black color in Figure 4.5(c), were identified by using the MTMF-based method. To assess the detection accuracy, the retrieved poppy field distribution map was compared against a poppy field distribution map of Nangarhar Province (Figure 4.5(a)) included in "Afghanistan Opium Survey 2004" (UNODC, 2004). The latter was interpreted by UNODC from 10 meter resolution SPOT-5 multi-spectral image pairs, acquired in both pre- and post-harvest seasons. It was the only one available to this study that could be used as groundtruth data.

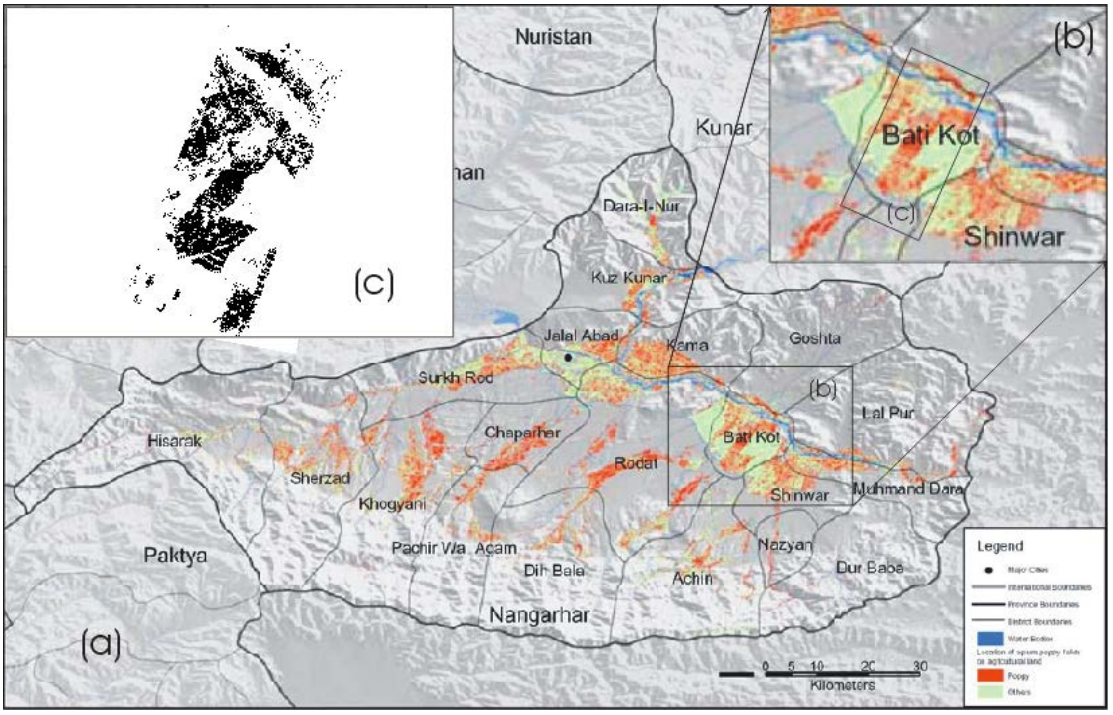

Figure 4.5 Poppy field distribution comparison. (a) Poppy field distribution map of Nangarhar Province, Afghanistan, reproduced from "Afghanistan Opium Survey 2004" (UNODC, 2004). The red and green colors represented poppy fields and other vegetation fields, respectively. (b) Poppy field distribution map of the Bati Kot study area, enlarged from (a). (c) Poppy field distribution map of the Bati Kot study area retrieved from an EO-1 Hyperion image over the study area acquired on March 21, 2004. The black color represented poppy fields in (c).

Quantitative detection accuracies of poppy fields could not be computed directly for the study area of Bati Kot due to the too coarse spatial resolution of Figure 4.5(b). Nevertheless, it is clear that the poppy field distribution retrieved in this study (Figure 4.5(c)) looked quite similar to the interpretation of UNODC (2004) (Figure 4.5(b)). Only in the bottom-right corner of the Bati Kot study area, poppy pixels seemed to be overestimated a little bit. Hence, the unsupervised MTMF-based method proposed from the Southwest Afghanistan seemed effective to detect poppy fields in the East Afghanistan, too.

4.5 Discussion and Conclusions

It is critical to find a practical and economical way to map poppy fields in Afghanistan under the strict constraints of inaccessibility of field surveys as well as of financial limitation. EO-1 Hyperion hyperspectral imagery used in this study is free of charge, but it has a coarse spatial resolution (i.e., 30 m × 30 m) relative to poppy fields (about 15 m × 15 m or less to 100 m × 100 m) in Afghanistan. Hence, spectral mixture analysis (SMA) was conducted to the Hyperion imagery using the MTMF in this study. Accurate endmember selection is a prerequisite for effective spectral unmixing. Endmembers of main vegetations must be determined from the Hyperion image itself because training samples were extremely difficult to obtain through field surveys due to security reasons in Afghanistan. In the MTMF-based method, endmembers were determined using the n-Dimensional Visualizer in ENVI. Three distinct clusters representing endmembers of poppy, wheat and tree, respectively were displayed clearly in the n-Dimensional Visualizer. The MTMF-based method discriminated the endmembers of main vegetations from the Hyperion image directly as effectively as it

did in the central Helmand Province in Wang et al. (2013b) although the two study areas were located in different environments and consisted of different number of main vegetation components. In addition, the MTMF-based method does not need to determine the endmembers of non-vegetation as the MTMF is a partial SMA. This also reduces the computational time needed in spectral umixing.

The comparison of the retrieved poppy field distribution map against groundtruth data showed that the MTMF-based method performed well in a river floodplain in mountainous East Afghanistan in this study. In addition, the method has been demonstrated effective in the arid plateau in southwest Afghanistan (Wang et al., 2013b). Therefore, this method was demonstrated practical in both of the two main environmental types in Afghanistan (Wikipedia, 2013). Moreover, the two studies involved two different years, i.e., 2009 and 2004, respectively. Therefore, the MTMF-based method may help better understand the temporal changes of poppy cultivation during the past decade in Afghanistan from the archives of EO-1 Hyperion images.

This unsupervised image-based and computationally efficient method was run aided by ENVI/IDL. In future research, an ENVI plugin will be built to help the users who are not an ENVI/IDL expert to apply this method easily to detect poppy fields directly from EO-1 Hyperion imagery in Afghanistan.

Acknowledgements

This work was supported by the Canada Research Chairs Program.

References

Datt, B., T.R. McVicar, T.G. Van Niel, D.L.B. Jupp, and J.S. Pearlman (2003). "Preprocessing EO-1 Hyperion Hyperspectral Data to Support the Application of Agricultural Indexes." *IEEE Transactions on Geoscience and Remote Sensing*, Vol. 41, No. 2, pp. 1246-1259.

Han, T., D.G. Goodenough, A. Dyk, and J. Love (2002). "Detection and correction of abnormal pixels in Hyperion image." *IEEE International Geoscience and Remote Sensing Symposium*, Vol. III, Toronto, ON, Canada, 1327–1330.

Jupp, D.L.B., B. Datt, T.R. McVicar, T.G. Van Niel, J.S. Pearlman, J.L. Lovell, and E.A. King (2003). "Improving the analysis of Hyperion red-edge index from an agricultural area." *Proceedings of SPIE*, Vol. 4898, pp. 1-15.

Lowe, A. (2010). "Remote Sensing based Monitoring of Opium Cultivations in Afghanistan." Master dissertation, University of Bonn, 106 p.

Manolakis, D. (2002). "Detection Algorithms for Hyperspectral Imaging Applications," *Project Report HTAP-8*, Lincoln Labs, Massachusetts Institute of Technology, Lexington Massachusetts.

Noujdina, N.V., and S.L. Ustin (2008). "Mapping Downy Brome (Bromus tectorum) using multidate AVIRIS data." *Weed Science*, Vol. 56, pp. 173–179.

Taylor, J.C., T.W. Waine, G.R. Juniper, D.M. Simms, and T.R. Brewer (2010). "Survey and monitoring of opium poppy and wheat in Afghanistan: 2003-2009." *Remote Sensing Letters*, Vol. 1, No. 3, pp. 179–185.

Tian Y.C., B.F. Wu, L. Zhang, Q.Z. Li, K. Jia, and M.P. Wen (2011). "Opium poppy monitoring with remote sensing in North Myanmar." *International Journal of Drug Policy*, Vol. 22, pp. 278–284.

Tsai, F., E.-K. Lin, and K. Yoshino (2007). "Spectrally segmented Principal Component Analysis of hyperspectral imagery for mapping invasive plant species." *International Journal of Remote Sensing*, Vol. 28, pp. 1023–1039.

UNODC (2004). "Afghanistan Opium Survey 2004." [Online] October 16, 2012: http://www.unodc.org/pdf/afg/afghanistan_opium_survey_2004.pdf.

UNODC (2005). "Afghanistan Opium Survey 2009." [Online] October 16, 2012: http://www.unodc.org/documents/crop-monitoring/Afghanistan/afg_survey_2005.pdf.

UNODC (2009). "Afghanistan Opium Survey 2009." [Online] October 16, 2012: http://www.unodc.org/documents/crop-monitoring/Afghanistan/Afgh-opiumsurvey2009_web.pdf.

Wang, J.J., Y. Zhang, and C. Bussink (2013a). "Remote Sensing of Opium Poppy Fields Using EO-1 Hyperion Hyperspectral Data: an Example in Afghanistan." *Proceedings of the 2013 Canadian Institute of Geomatics Annual Conference and the 2013 International Conference on Earth Observation for Global Changes (EOGC'2013)*, 5-7 June 2013, Toronto, Ontario, Canada, pp. 106-110.

Wang, J.J., Y. Zhang, and C. Bussink (2013b) "An unsupervised MTMF-based method for detecting opium poppy fields in Helmand, Afghanistan, from EO-1 Hyperion data." (submitted to *International Journal of Remote Sensing*)

Wikipedia (2013). "Geography of Afghanistan." [Online] July 10, 2013: http://en.wikipedia.org/wiki/Geography_of_Afghanistan.

CHAPTER 5

CAN EO-1 ALI DATA DETECT OPIUM POPPY FIELDS IN HELMAND, AFGHANISTAN?

* This paper is co-authored by Wang, J.J., Zhang, Y. and Bussink, C., and it will be submitted to *Remote Sensing (peer-reviewed Open Access journal).*

Abstract

Timely and accurately detection of poppy fields is critical for fighting against the opium production effectively. To overcome the constraints of inaccessibility of poppy fields in some countries like Afghanistan, high-resolution multispectral satellite images ($\leq$ 1m) images like pan-sharpened IKONOS have been applied by some organizations such as United Nations Office on Drugs and Crime. However, their high prices prevent them from working for a large area. Wang et al. (2013a, 2013b) have demonstrated that moderate spatial resolution EO-1 Hyperion hyperspectral data, free of charge, could map poppy fields in a study area located in central Helmand, Afghanistan even if training samples were unavailable. In comparison to the hyperspectral data, moderate spatial resolution multispectral satellite imagery is easier to obtain and to process, and it has been employed in target detection in existing literature, Therefore, this study, taking moderate spatial resolution EO-1 Advanced Land Imager (ALI) multispectral imagery as

an example, investigated if this imagery could map poppy fields in the same study area using the same methodology as in Wang et al. (2013b). It was found that the ALI data could not produce reasonable detection of poppy fields in the study area.

Keywords: poppy detection, multispectral imagery, EO-1 Advanced Land Imager (ALI), Afghanistan

5.1 Introduction

Fighting against the opium production effectively is a tough task for international societies. In fact, even how to timely and accurately investigate where opium poppy fields are is a challenge. In general, they are located at the places that are difficult to reach due to extremely bad transportation conditions. Moreover, it even can be a quite dangerous task to visit the poppy fields in some countries or regions like Afghanistan due to security reasons although the country has become the dominant illicit opium producer in the entire world (UNODC, 2011; UNODC, 2012).

With the recent surge in the availability of spectral imaging sensors, the technology of remote sensing offers a potential way to map vegetation and detect plant species (e.g., Everitt et al., 1996; Langley et al., 2001; Nordberg and Evertson, 2003; Bradley and Mustard, 2005; Walsh et al., 2008; Groeneveld and Watson, 2008; Xie et al., 2008; Wilfong et al., 2009; Gavier-Pizarro et al., 2012; Padalia et al., 2013). However, remote sensing of opium poppy fields is still a big challenge because it is often too difficult and even dangerous to obtain training samples through field surveys.

Although satellite images have been used to overcome the constraints of inaccessibility of poppy field surveys (e.g., UNODC, 2009; Taylor et al., 2010; Tian et al., 2011), the main spectral data sources were expensive high spatial resolution multispectral images (≤ 1m) like pan-sharpened IKONOS, QuickBird, etc. These expensive images were not appropriate for developing countries like Afghanistan. Hence, Wang et al. (2013a, 2013b) have attempted to use free EO-1 Hyperion hyperspectral data to detect poppy fields in a study area located in central Helmand Province in Afghanistan. They proposed two unsupervised methods that employed two different approaches, i.e., Multiple Endmember Spectral Mixture Analysis (MESMA; Roberts et al., 1998) and Mixture Tuned Matched Filtering (MTMF; Boardman, 1998), respectively to conduct spectral unmixing. Both of the two methods did not require training samples, and they performed well even if only little prior knowledge of the study area was available. The two methods produced similar detection accuracies of poppy fields, but the MTMF-based one had much higher computational efficiency because it only needed to work on several Minimum Noise Fraction (MNF) bands.

The hyperspectral data are more difficult to obtain and to process in comparison to multispectral data. However, it is not clear if poppy fields can also be detected effectively from moderate spatial resolution multispectral data. In existing literature, moderate spatial resolution multispectral images have also been employed in target detection using the MTMF. For instance, Pal et al. (2011) used Landsat ETM+ data to map mineral occurrences in India, Sankey and Glenn (2011) used Landsat-5 TM together with LiDAR fusion for sub-pixel Juniper tree cover estimates in United States, Hassan and Hashim (2011) used the MTMF to decompose mixed pixels of ASTER

satellite data for mapping Chengal (Neobalanocarpus heimii sp) Tree in Malaysia, and Pour and Hashim (2012) distinguished the phyllic, argillic and propylitic alteration zones of porphyry copper mineralization using ASTER data in Iran.

Therefore, this study aimed to investigate if moderate spatial resolution multispectral data could detect opium poppy fields by using the MTMF-based method (Wang et al., 2013b), and then to compare the performance of the multispectral data with that of hyperspectral data. A study area in the central Helmand Province, Afghanistan (Figure 5.1) that was used in Wang et al., 2013b) was also used in this study.

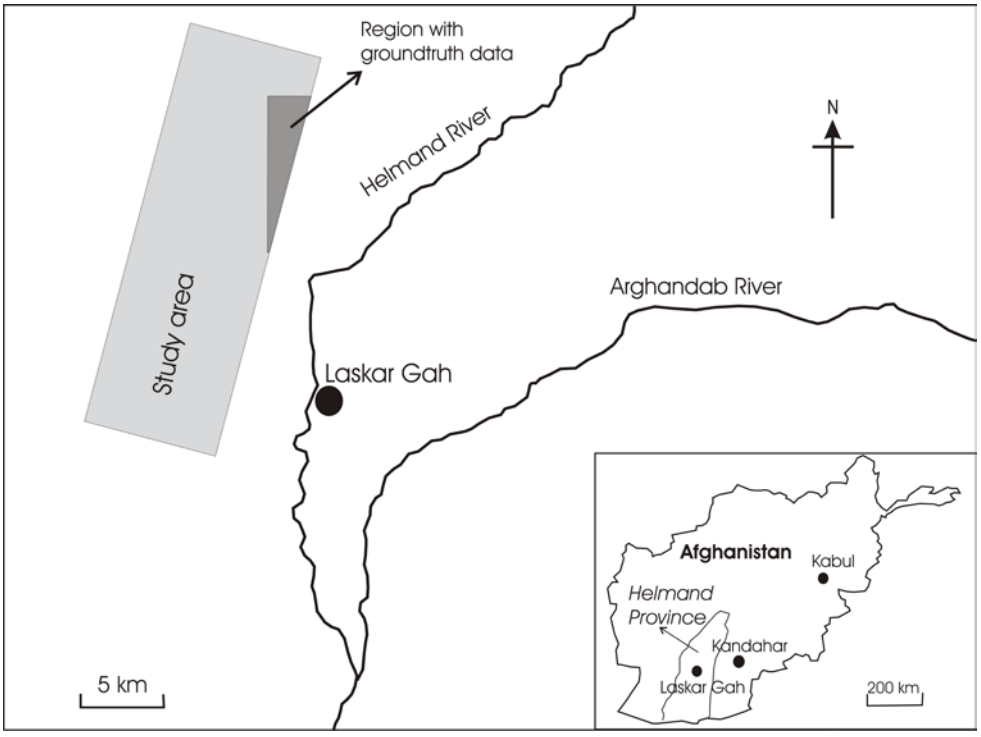

Figure 5.1 Study area map

5.2 Data and Methodology

5.2.1 Data

An interpretation of opium fields provided by the United Nations Office on Drugs and Crime (UNODC) was used as surrogate groundtruth data in this study. The interpretations were part of "Opium Poppy Survey 2009" conducted by UNODC and Ministry of Counter Narcotics of Afghanistan. It was based on an IKONOS image acquired on April 11, before harvest season, in 2009.

An EO-1 Advanced Land Imager (ALI) image over the study area was acquired on March 11, 2009, the same time as the EO-1 Hyperion image that was used in Wang et al. (2013b). All nine of the ALI image's 30 m resolution multispectral bands were used to detect poppy fields in this study. The image was processed to Standard Terrain Correction (Level 1T) before being downloaded from the USGS website. This study used a Landsat ETM+ image acquired on April 23, 2009 to geometrically correct the ALI image.

5.2.2 Methodology

The MTMF-based method used (Wang et al., 2013b) is described as follows. The detection accuracy was assessed by comparing with the surrogate ground truth data of poppy field provided by UNODC pixel by pixel.

5.2.2.1 ALI Multispectral Data Pre-processing

The pre-processing of ALI data was different from that of Hyperion data. The digital numbers were converted into radiance values by using the multiplicative factors and the additive factors of each band (Chander et al., 2009). Radiance of all nine multispectral bands was input into the Fast Line-of-sight Atmospheric Analysis of Spectral Hypercubes (FLAASH), an atmospheric correction module implemented in the ENVI software (ITT Visual Information Solutions, Boulder, CO, USA) to calibrate the at-sensor radiance data to land surface reflectance. The FLAASH model was run following the "ENVI FLAASH Module User's Guide" (ITT Visual Information Systems, 2006). As ALI level L1T data are in units of $W/(m^2\ sr\ \mu m)$ while the FLAASH atmospheric correction software uses units of $\mu W/(cm^2\ sr\ nm)$, the scale factors 10 were used when running the FLAASH model.

The projection of the ALI L1T data was UTM 41N, datum WGS 84. Geometric correction was conducted on the atmospherically corrected ALI image by using the ENVI software by collecting 31 ground control points (GCPs) in reference to the Landsat 7 ETM+ imagery acquired on April 23, 2009 over the study area. An overall root mean square error (RMSE) of 0.15 pixel was achieved.

5.2.2.2 Endmember Determination

Only the pixels with Normalized Difference Vegetation Index (NDVI) values greater than 0 were used to determine endmembers (see Appendix I). NDVI values were computed from ALI Band 5 (662.00 nm) and Band 6 (790.00 nm) for each pixel. A Minimum Noise Fraction (MNF) transform in the ENVI was conducted to determine the

inherent dimensionality of image data, and to segregate noise in the data (Boardman and Kruse, 1994). The inherent dimensionality of the data was determined by examining the final eigenvalues and the associated images. In this study, only the first four MNF bands with high eigenvalues were used in following stages because the other MNF bands carried too many noises.

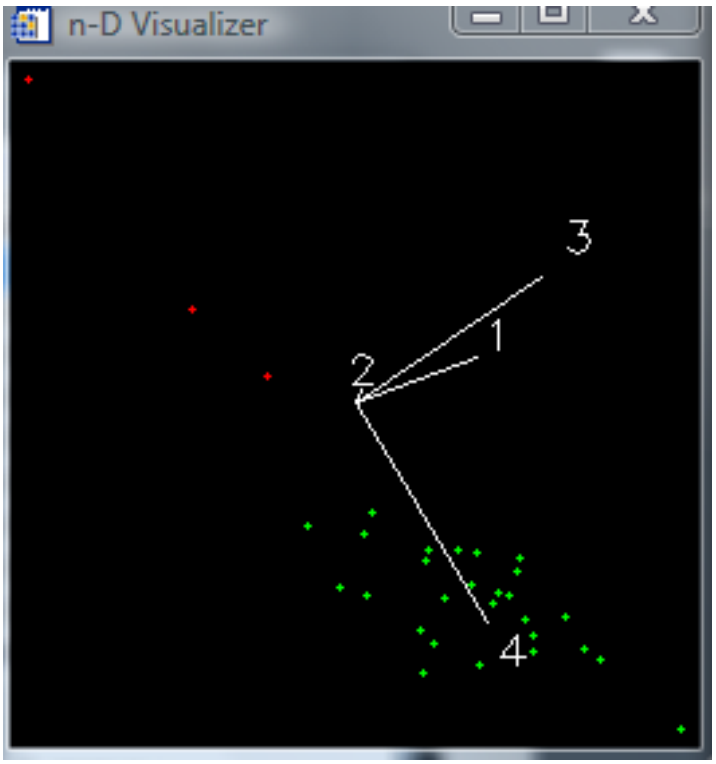

Figure 5.2 The 30 pure vegetation pixels with NDVI ≥0.2 and with smaller reflectance at ALI Band 5 (red) than at Band 4 (green) formed two vegetation clusters, Components A (top left) and B (bottom right) in the n-Dimensional Visualizer in ENVI. Numbers 1-4 referred to MNF band numbers.

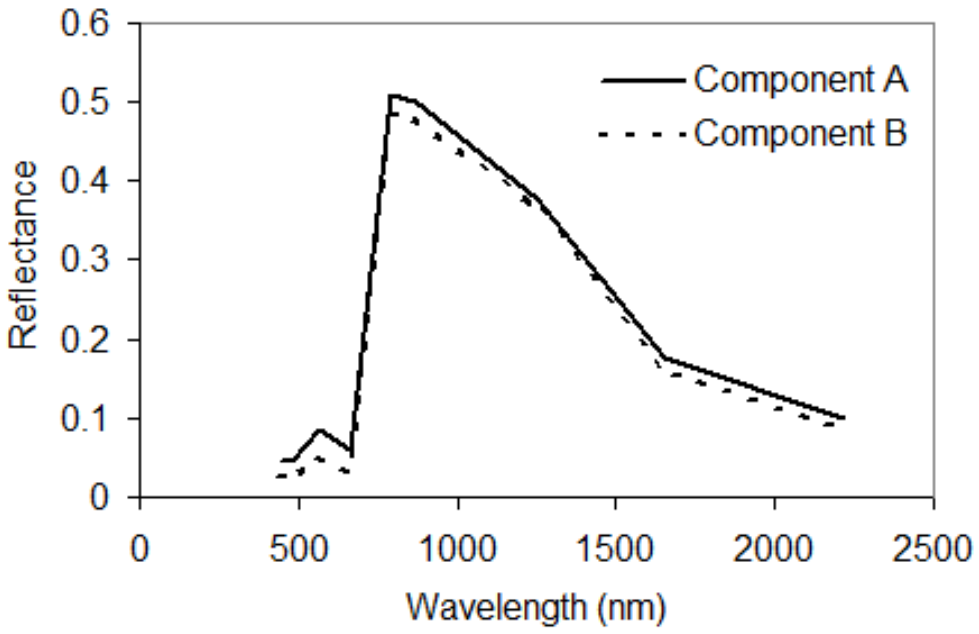

Figure 5.3 Spectral profile of averaged reflectance of endmembers in the two vegetation clusters, i.e., Components A (poppy) and B (wheat), respectively.

Next, Pixel Purity Index (PPI) values were computed from the MNF output by using the ENVI software to represent the pixels with higher purity and spectral extremity. Only the 65 pixels with PPI values not less than 2000 were used to determine endmembers. Then, the 29 pixels whose NDVI values were greater than 0 and less than 0.2 were seen as non-vegetation pixels (Tsai et al., 2007; Noujdina and Ustin, 2008). Among the 36 pixels with NDVI values not less than 0.2, six pixels were not involved in further analysis. These six pixels were mixed pixels of vegetation with non-vegetation because the reflectance at Band 5 (red) was smaller than that at Band 4 (green) for pure vegetation pixels due to the absorption of light by chlorophyll in the red region. The other 30 pixels were input into the n-Dimensional Visualizer in the ENVI for the clustering process, which clustered the 30 pixels into two groups (Figure 5.2)

representing two kinds of vegetations as shown in Figure 5.3. The two main crops were poppy and wheat at the season in the study area in 2009, and poppy had lower NDVI value than wheat (UNDOC, 2009; Lowe, 2010). Component A with 3 endmembers should be poppy because its NDVI was 0.79, lower than Component B, with 27 endmembers, whose NDVI value was 0.88.

5.2.2.3 Poppy Pixels Determination

An average MNF-transformed spectral library was built for each component (i.e., poppy and wheat) by using the ENVI software. The MTMF model of ENVI was run on the MNF-transformed ALI image using each component of poppy and wheat as target, respectively.

The MTMF output two sets of images, i.e., MF score image and Infeasibility image. Then, three filters that were used in Wang et al. (2013b) were also used to each pixel in this study: (1) MF > -0.2, (2) Infeasibility < 6, and (3) NDVI ≥ 0.2. The remaining pixels were determined as poppy pixels if their MF values of poppy were higher than their MF values of wheat.

5.3 Results and Discussion

This study resulted in poppy field distribution according to the ALI image acquired on March 11, 2009 in the study area. Figure 5.4(a) displayed the distribution of poppy fields retrieved by this study. In comparison to the surrogate groundtruth data (Figure 4(b)) provided by UNODC, the number of poppy pixels was largely underestimated.

Such underestimation was more significant in the north part of the study area. On the contrary, Wang et al. (2013b) that employed Hyperion hyperspectral data produced a distribution map of poppy fields that was highly similar to the surrogate groundtruth data although the same MTMF-based method was applied by both studies.

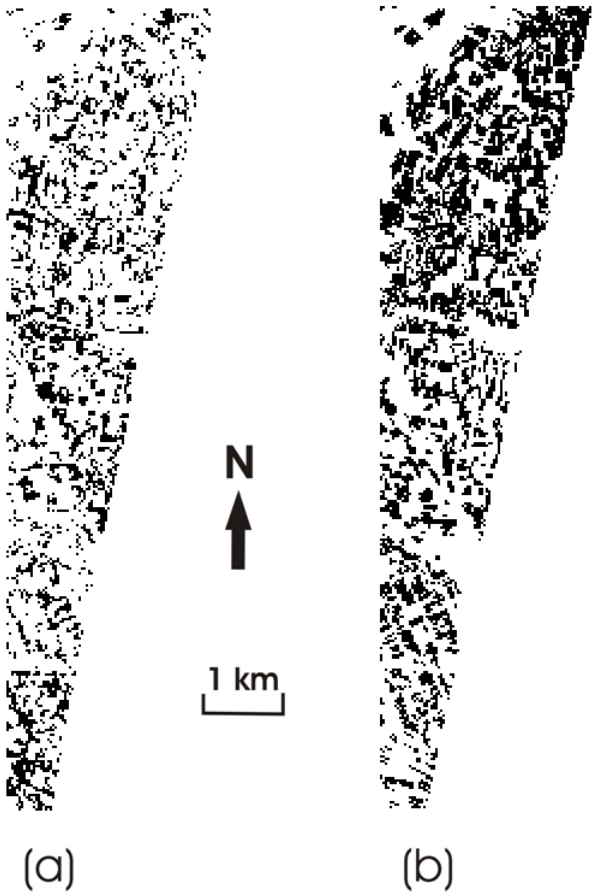

Figure 5.4 Poppy distribution maps over the study area that were (a) retrieved from an EO-1 ALI image acquired on March 11, 2009, and (b) provided by UNODC.

Accuracy assessment, which was done pixel by pixel, was used to quantify how well poppy fields were detected from EO-1 ALI data. This produced producer's accuracy of 32% and user's accuracy of 54%, respectively. This meant that 68% of true poppy pixels were identified as non-poppy pixels, while 46% of the pixels that were identified as poppy fields were not real ones. The overall accuracy was 63%. The kappa coefficient was 0.15, indicating a slight agreement between retrieved poppy field and surrogate groundtruth data. Therefore, it was clear that ALI data failed in detection of poppy fields.

In contrast, Wang et al. (2013b) achieved producer's accuracy of 61%, user's accuracy of 73%, and overall accuracy of 76%, respectively by using EO-1 Hyperion data to detect poppy fields in the same study area for the same date. Wang et al. (2013b) also produced kappa coefficient of 0.48, indicating a moderate agreement. Therefore, Hyperion hyperspectral data performed much better than ALI multispectral data did, although they had the same moderate spatial resolution of 30 m.

A possible reason was that Wang et al. (2013b) applied 121 bands of Hyperion hyperspectral data that had much more bands with much higher spectral resolution, while this study applied only nine bands of ALI multispectral data. Hyperspectral data having a large number of bands with narrow spectral interval provide almost continuous spectra of targets and natural backgrounds, and this may increase the detection capability of subpixel size targets (Manolakis, 2002). Consequently, poppy fields could be better identified from Hyperion hyperspectral data.

In addition, in Wang et al. (2013b) that used hyperspectral data, vegetation endmembers were divided into two quite distinct vegetation clusters, i.e., poppy cluster and wheat cluster. However, this study was different. As shown in Figure 5.2, the 30 vegetation endmembers did not show distinct clusters. Moreover, the three endmembers of the poppy component also did not form a significant and tight cluster. Therefore, the difference between the poppy component and the wheat component could be identified more accurately from hyperspectral data rather than from multispectral data, and this likely led to higher accuracies of poppy field detection in Wang et al. (2013b), too.

5.4 Conclusions

This study investigated if moderate spatial resolution EO-1 ALI multispectral imagery could map poppy fields in a study area located in central Helmand, Afghanistan using the MTMF-based method (Wang et al., 2013b) considering this imagery was easier to obtain (wider swath) and to process than the Hyperion hyperspectral imagery. By comparing the retrieved poppy field distribution against surrogate groundtruth data pixel by pixel, the resultant detection accuracies were so low that the ALI multispectral data could not produce effective detection of poppy fields in the study area.

A comparison of this study that employed an ALI multispectral image with Wang et al. (2013b) that employed a Hyperion hyperspectral image demonstrated that hyperspectral data produced more accurate detection of poppy fields, although the two images were acquired on the same date, and the two studies applied the same method (i.e., MTMF-based) and selected the same study area.

Acknowledgements

This work was supported by the Canada Research Chairs Program. The authors thank the United Nations Office on Drugs and Crime (UNODC) for providing the interpretation files of opium fields. The views expressed in this paper are those of the author(s) and do not necessarily reflect the views of the United Nations.

References

Boardman, J. W., and F.A. Kruse (1994). "Automated spectral analysis: A geologic example using AVIRIS data, north Grapevine Mountains, Nevada." *Proceedings, Tenth Thematic Conference on Geologic Remote Sensing*, Environmental Research Institute of Michigan, Ann Arbor, MI, p. I-407 - I-418.

Boardman, J.W. (1998). "Leveraging the high dimensionality of AVIRIS data for improved sub pixel target unmixing and rejection of false positives; Mixture Tuned Matched Filtering." *Summaries of the 7th JPL Airborne Earth Science Workshop* (Jet Propulsion Laboratory Publication), 1, pp. 53.

Bradley, B.A., and J.F. Mustard (2005) "Identifying land cover variability distinct from land cover change: cheatgrass in the Great Basin." *Remote Sensing and Environment*, Vol. 94, pp. 204–213.

Chander, G., B.L. Markham, and D.L. Helder (2009). "Summary of current radiometric calibration coefficients for Landsat MSS, TM, ETM+, and EO-1 ALI sensors." *Remote Sensing of Environment*, Vol. 113, No. 5, pp. 893-903.

Everitt, J.H., D.E. Escobar, M.A. Alaniz, M.R. Davis, and J.V. Richerson (1996). "Using spatial information technologies to map Chinese tamarisk (Tamarix chinensis) infestations." *Weed Science*, Vol. 44, pp. 194–201.

Gavier-Pizarro, G.I., T. Kuemmerle, L.E. Hoyos, S.I. Stewart, C.D. Huebner, N.S. Keuler, and V.C. Radeloff (2012). "Monitoring the invasion of an exotic tree (Ligustrum lucidum) from 1983 to 2006 with Landsat TM/ETM+ satellite data and Support Vector Machines in Cordoba, Argentina." *Remote Sensing of Environment*, Vol. 122, pp. 134–145.

Groeneveld, D.P., and R.P. Watson (2008), "Near-infrared discrimination of leafless saltcedar in wintertime Landsat TM." *International Journal of Remote Sensing*, Vol. 29, pp. 3577–3588.

Hassan, N., and M. Hashim (2011). "Decomposition of mixed pixels of ASTER satellite data for mapping Chengal (Neobalanocarpus heimiisp) tree." Paper presented at 2011 IEEE International Conference on Control System, Computing and Engineering, ICCSCE 2011, November 25, 2011 -November 27, 2011, Penang, Malaysia, IEEE Computer Society.

ITT Visual Information Systems (2006). "ENVI FLAASH Module User's Guide (2006 Edition)." [Online] September 21, 2012: ftp://popo.jpl.nasa.gov/pub/ENVI_Installers/ENVI_Documentation/docs/FLAASH_Module.pdf.

Langley, S.K., H.M. Cheshire, and K.S. Humes (2001) "A comparison of single date and multitemporal satellite image classifications in a semi-arid grassland." *Journal of Arid Environments*, Vol. 49, pp. 401–411.

Lowe, A. (2010). "Remote Sensing based Monitoring of Opium Cultivations in Afghanistan." Master dissertation, University of Bonn, 106 p.

Manolakis, D. (2002). "Detection Algorithms for Hyperspectral Imaging Applications," *Project Report HTAP-8*, Lincoln Labs, Massachusetts Institute of Technology, Lexington Massachusetts.

Nordberg, M.L., and J. Evertson (2003) "Vegetation index differencing and linear regression for change detection in a Swedish mountain range using Landsat TM and ETM+ imagery." *Land Degradation & Development*, Vol. 16, pp. 139–149.

Noujdina, N.V., and S.L. Ustin (2008). "Mapping Downy Brome (Bromus tectorum) using multidate AVIRIS data." *Weed Science*, Vol. 56, pp. 173–179.

Padalia, H., M. Kudrat, and K.P. Sharma (2013). "Mapping sub-pixel occurrence of an alien invasive Hyptis suaveolens (L.) Poit. using spectral unmixing technique." *International Journal of Remote Sensing*, Vol. 34, No. 1, pp. 325-340.

Pal, S.K., T.J. Majumdar, A.K. Bhattacharya, and R. Bhattacharyya (2011). "Utilization of Landsat ETM+ data for mineral-occurrences mapping over Dalma and Dhanjori, Jharkhand, India: an Advanced Spectral Analysis approach." *International Journal of Remote Sensing*, Vol. 32, No. 14, pp. 4023-4040.

Pour, A.B., and M. Hashim (2012). "Identifying areas of high economic-potential copper mineralization using ASTER data in the Urumieh–Dokhtar Volcanic Belt, Iran." *Advances in Space Research*, Vol. 49, pp. 753–769.

Roberts, D.A., M. Gardner, R. Church, S. Ustin, G. Scheer, and R.O. Green (1998). "Mapping Chaparral in the Santa Monica Mountains using Multiple Endmember

Spectral Mixture Models." *Remote Sensing of Environment*, Vol. 65, pp. 267−279.

Sankey, T., and N. Glenn (2011). "Landsat-5 TM and LiDAR fusion for sub-pixel Juniper tree cover estimates in a western rangeland." *Photogrammetric Engineering & Remote Sensing*, Vol. 77, No. 12, pp. 1241-1248.

Taylor, J.C., T.W. Waine, G.R. Juniper, D.M. Simms, and T.R. Brewer (2010). "Survey and monitoring of opium poppy and wheat in Afghanistan: 2003-2009." *Remote Sensing Letters*, Vol. 1, No. 3, pp. 179–185.

Tian Y.C., B.F. Wu, L. Zhang, Q.Z. Li, K. Jia, and M.P. Wen (2011). "Opium poppy monitoring with remote sensing in North Myanmar." *International Journal of Drug Policy*, Vol. 22, pp. 278–284.

Tsai, F., E.-K. Lin, and K. Yoshino (2007). "Spectrally segmented Principal Component Analysis of hyperspectral imagery for mapping invasive plant species." *International Journal of Remote Sensing*, Vol. 28, pp. 1023–1039.

UNODC (2009). "Afghanistan Opium Survey 2009." [Online] October 16, 2012: http://www.unodc.org/documents/crop-monitoring/Afghanistan/Afgh-opiumsurvey2009_web.pdf.

UNODC (2011). "Afghanistan Opium Survey 2011." [Online] October 16, 2012: http://www.unodc.org/documents/crop-monitoring/Afghanistan/Afghanistan_opium_survey_2011_web.pdf.

UNODC (2012). "World Drug Report 2012." [Online] July 27, 2013: http://www.unodc.org/documents/data-and-analysis/WDR2012/WDR_2012_web_small.pdf.

Walsh, S.J., A.L. McCleary, C.F. Mena, Y. Shao, J.P. Tuttle, A. Gonzalez, and R. Atkinson (2008). "QuickBird and Hyperion data analysis of an invasive plant species in the Galapagos Islands of Ecuador: implications for control and land use management." *Remote Sensing of Environment*, Vol. 112, pp. 1927–1941.

Wang, J.J., Y. Zhang, and C. Bussink (2013a). "Remote Sensing of Opium Poppy Fields Using EO-1 Hyperion Hyperspectral Data: an Example in Afghanistan." *Proceedings of the 2013 Canadian Institute of Geomatics Annual Conference and the 2013 International Conference on Earth Observation for Global Changes (EOGC'2013)*, 5-7 June 2013, Toronto, Ontario, Canada, pp. 106-110.

Wang, J.J., Y. Zhang, and C. Bussink (2013b) "An unsupervised MTMF-based method for detecting opium poppy fields in Helmand, Afghanistan, from EO-1 Hyperion data." (submitted to *International Journal of Remote Sensing*)

Wilfong, B.N., D.L. Gorchov, and M.C. Henry (2009) "Detecting an invasive shrub in deciduous forest understories using remote sensing." *Weed Science*, Vol. 57, pp. 512–520.

Xie, Y. (2008) "Remote sensing imagery in vegetation mapping: A review." *Journal of Plant Ecology*, Vol. 1, No. 1, pp. 9-23.

CHAPTER 6

CONCLUSIONS AND RECOMMENDATIONS

This chapter summarized this MScE research that aimed to achieve the objective of finding a way to detect poppy fields in Afghanistan under some limits or circumstances that were typical to Afghanistan. Then, the contributions of this research were highlighted. Finally, several recommendations were outlined for future studies.

6.1 Summary of the Research

In Chapter 1, this thesis introduced the problem of opium poppy, especially the opium problem in the Afghanistan. The widely planted opium poppy in this country highlighted the necessity of timely monitoring of poppy fields through remote sensing. The literature review of remote sensing of poppy fields identified an important and urgent research problem: how to remotely detect the poppy fields effectively in Afghanistan, where opium poppy is widely planted, field survey is quite dangerous, and financial support is limited? Therefore, this thesis aimed to find a way to detect effectively opium poppy fields in Afghanistan from EO-1 Hyperion hyperspectral data that are free of charge. Such a method must be unsupervised as no training samples are available, and computational efficient as it should work for a huge area. In addition, the method cannot use image pairs acquired pre- and post-harvest seasons, respectively because poppy fields must be detected before harvest for timely poppy eradication. Considering its high prices, high spatial resolution imagery is not suitable for Afghanistan although it was the main data source in previous studies.

In Chapter 2 (Wang et al., 2013a), an unsupervised Multiple Endmember Spectral Mixture Analysis (MESMA)-based method was proposed. Endmembers (see Appendix I) of main crop components were determined first although no training samples were used and only general information of the study area was available. Then, the MESMA decomposed mixed pixels to identify poppy fields.

Although the MESMA-based method could detect the poppy fields, the method is computationally expensive because it works on all 121 used spectral bands. Hence, Chapter 3 (Wang et al., 2013b) proposed an unsupervised Mixture Tuned Matched Filtering (MTMF)-based method. This method has higher computational efficiency than the MESMA method because this MTMF-based one only works on the first five Minimum Noise Fraction (MNF) bands. They both achieved similar detection accuracies.

In both Chapters 2 and 3, a place on the arid plateau in central Helmand Province in southwest Afghanistan was used as a study area. Research in Chapter 4 (Wang and Zhang, 2013) selected a place in the floodplain of Kabul River in mountainous east Afghanistan to further test the MTMF-based method for another year. More main vegetation components were involved in the detection. The detected poppy field distribution seemed reasonable and consistent with results by using high spatial resolution images in UNODC (2004).

All of Chapters 2-4 applied EO-1 Hyperion hyperspectral data. Taking EO-1 Advanced Land Imager (ALI) data as an example, Chapter 5 (Wang et al., 2013c) demonstrated that moderate spatial resolution multispectral data could not provide acceptable poppy field distribution, although moderate resolution multispectral data are

easier to obtain as well as to process, and although they have been used in target detection in previous studies, too.

6.2 Contributions of the Research

The major contribution of this thesis is that two unsupervised methods (i.e., a MESMA-based one and a MTMF-based one) were proposed, and they both could detect poppy fields in Afghanistan from satellite hyperspectral images directly. Moreover, the MTMF-based method performed well in both of the two main environments in Afghanistan.

Neither of the two methods requires training samples. They could determine endmembers of main components directly from the imagery itself with only little general priori knowledge of the study area. Moreover, users do not have to assume the number of classes in an image that is required by conventional unsupervised methods. This is critical because training samples are extremely difficult to obtain in Afghanistan, and sometime it is unfeasible to conduct field surveys in some regions in this country due to security reasons.

In the MESMA-based method, it was found that using 2- and 3-endmember models led to higher detection accuracies of poppy fields than involving 4-endmember model in the methodology. It was also found that introducing a RMSE difference threshold of reflectance (i.e., >0.05%) could increase detection accuracies significantly in the study area.

In the MTMF-based method, it was found that, although it is commonly accepted that the pixels with zero or negative Matched Filtering (MF) scores should be seen as background when running the MTMF model, simply ignoring these pixels could largely reduce producer's accuracy and kappa coefficient in poppy field detection. A possible reason may be the high spectral similarity between poppy and wheat. No similar report was found in literature review.

The two methods could achieve similar detection accuracies although the MTMF-based one could provide higher user's accuracy. However, the MTMF-method is more computationally efficient because it works on only the first several MNF bands while the MESMA-based one works on over one hundred of spectral bands. Faster detection is important to huge area.

To the authors' knowledge, there is little evidence that aerial and/or satellite hyperspectral data have been used to detect poppy fields in previous studies. This thesis employed spaceborne EO-1 Hyperion hyperspectral imagery. The Hyperion imagery is free of charge. This makes it possible to cover the widely distributed poppy fields in Afghanistan. In contrast, high spatial resolution satellite imagery and aerial hyperspectral data with high spatial resolution are too expensive for this developing country if without foreign financial aids.

In addition, taking 30 m EO-1 ALI data as an example, this thesis demonstrated that moderate spatial resolution multispectral imagery could not detect poppy fields effectively in Afghanistan, although moderate spatial resolution multispectral data are easier to obtain and to process.

6.3 Recommendations for Further Research

The research related to this thesis found that pure poppy pixels were visibly different from pure wheat pixels; however, mixed poppy pixels and mixed wheat pixels showed high spectral similarity. This was the main reason for detection errors of poppy fields in study areas. In the flowering season of poppies, the spectral difference between mixed poppy pixels and mixed wheat pixels may be bigger because poppy was spectrally more different from a range of other crops in the flowering stage (Sader, 1991; Taylor et al., 2010; Jia et al., 2011). Hence, it is recommended to try using images acquired in the flowering season to increase detection accuracy of poppy fields where they are available.

UNODC used a pair of IKONOS satellite images collected at two stages, namely the pre-harvest (capsule) stage and the post-harvest (post-lancing) stage, because poppy fields are ploughed immediately after the harvest, whereas wheat fields are not (UNODC, 2009). This thesis did not apply a pair of images because our objective was to detect poppy fields before harvest which was necessary for poppy eradication. To investigate the area of poppy cultivation, it is recommended to apply a pair (pre- and post-harvest) of EO-1 Hyperion hyperspectral images in future research. Increase of poppy field detection accuracy is expected.

It is recommended to write an ENVI plugin for poppy field detection from EO-1 Hyperion data by using the MTMF-based method. This may help the users who are not an ENVI/IDL expert to apply this method easily, from pre-processing of EO-1 Hyperion data to retrieving the distribution of poppy fields in Afghanistan.

In addition, it is recommended to improve the performance of the MTMF-based method on poppy field detection through image fusion of Hyperion and ALI images. Both Hyperion and ALI sensors are carried by the EO-1 platform. Having both Hyperion and ALI on the same platform reduces temporal effects on registration accuracy greatly. Hyperion data have high spectral resolution, but its spatial resolution is only 30 m. As the ALI panchromatic band has higher spatial resolution (10 m), previous studies like Memarsadeghi et al. (2005), Capobianco et al. (2007), Pour and Hashim (2013) have enhanced Hyperion hyperspectral data's spatial resolution through fusing Hyperion with ALI Panchromatic image.

In addition, it is too early to say if this method is also suitable for other opium poppy producing regions outside of Afghanistan. The crops that co-exist with the poppy may be different in other countries. Moreover, poppy fields larger than one pixel may be unavailable, so pure poppy pixels may be unavailable within an entire Hyperion image. Therefore, if groudtruth data obtained from field surveys are available in other countries, further testing if this sensor under the different conditions noted would be very useful in assessing the applicability of this approach to different regions.

References

Capobianco, L., A. Garzelli, L.A. Filippo Nencini, and S. Baronti (2007). "Spatial enhancement of Hyperion hyperspectral data through ALI panchromatic image." *IEEE International Geoscience and Remote Sensing Symposium (IEEE, 2007),* 5158–5161.

Jia, K., B. Wu, Y. Tian, Q. Li, and X. Du (2011). "Spectral discrimination of opium poppy using field spectrometry." *IEEE Transactions on Geoscience and Remote Sensing*, Vol. 49, No. 9, pp. 3414-3422.

Memarsadeghi, N., J. Le Moigne, D.M. Mount, and J. Morisette (2005). "A new approach to image fusion based on cokriging." *Proceedings of The Eight International Conference on Information Fusion (Fusion 2005)*, Philadelphia, PA, 2005, 1, 622-629.

Pour, A.B., and M. Hashim (2013). "Fusing ASTER, ALI and Hyperion data for enhanced mineral mapping." *International Journal of Image and Data Fusion*, Vol. 4, No. 2, pp. 126-145.

Sader, S.A. (1991). "Remote Sensing of Narcotic Crops with special reference to techniques for detection and monitoring of poppy production in Afghanistan." [Online] June 9, 2013: http://pdf.usaid.gov/pdf_docs/PNABT431.pdf.

Taylor, J.C., T.W. Waine, G.R. Juniper, D.M. Simms, and T.R. Brewer (2010). "Survey and monitoring of opium poppy and wheat in Afghanistan: 2003-2009." *Remote Sensing Letters*, Vol. 1, No. 3, pp. 179–185.

UNODC (2004). "Afghanistan Opium Survey 2004." [Online] October 16, 2012: www.unodc.org/pdf/afg/afghanistan_opium_survey_2004.pdf.

UNODC (2009). "Afghanistan Opium Survey 2009." [Online] October 16, 2012: http://www.unodc.org/documents/crop-monitoring/Afghanistan/Afgh-opiumsurvey2009_web.pdf.

Wang, J.J., Y. Zhang, and C. Bussink (2013a). "Remote Sensing of Opium Poppy Fields Using EO-1 Hyperion Hyperspectral Data: an Example in Afghanistan." *Proceedings of the 2013 Canadian Institute of Geomatics Annual Conference and the 2013 International Conference on Earth Observation for Global Changes (EOGC'2013)*, 5-7 June 2013, Toronto, Ontario, Canada, pp. 106-110.

Wang, J.J., Y. Zhang, and C. Bussink (2013b) "An unsupervised MTMF-based method for detecting opium poppy fields in Helmand, Afghanistan, from EO-1 Hyperion data." (submitted to *International Journal of Remote Sensing*)

Wang, J.J., and Y. Zhang (2013) "An unsupervised approach to detect opium poppy fields in Bati Kot, Nangarhar, Afghanistan, using EO-1 Hyperion data." (to be submitted to *Remote Sensing* (peer-reviewed Open Access journal))

Wang, J.J., Y. Zhang, and C. Bussink (2013c) "Can EO-1 ALI data detect opium poppy fields in Helmand, Afghanistan?" (to be submitted to *Remote Sensing* (peer-reviewed Open Access journal))

APPENDIX I

ENDMEMBER

For satellite images, the concept of “endmember” is related to the spectral mixture problem. When the spatial resolution of an image is not high enough to disparate materials, or when distinct materials are combined into a homogeneous mixture, there exist mixed pixels within the image that are a mixture of various distinct substances (Keshava and Mustard, 2002). The resulted spectral measurement will be some composite of the individual spectra of these distinct substances or materials. Thus, the pure spectral signatures, or the constituent spectra are defined as “endmembers” (Keshava and Mustard, 2002).

To decompose mixed pixels into respective endmembers and their abundances, spectral unmixing should be performed using various existing approaches. For example, Multiple Endmember Spectral Mixture Analysis (MESMA; Roberts et al., 1998) and Mixture Tuned Matched Filtering (MTMF; Boardman, 1998) are two popular spectral unmixing methods.

References

Boardman, J.W. (1998). "Leveraging the high dimensionality of AVIRIS data for improved sub pixel target unmixing and rejection of false positives; Mixture Tuned Matched Filtering." *Summaries of the 7th JPL Airborne Earth Science Workshop* (Jet Propulsion Laboratory Publication), 1, pp. 53.

Keshava, N., and J. F. Mustard (2002). “Spectral unmixing.” *IEEE Signal Processing Magazine*, Vol. 19, pp. 44–57.

Roberts, D.A., M. Gardner, R. Church, S. Ustin, G. Scheer, and R.O. Green (1998). "Mapping Chaparral in the Santa Monica Mountains using Multiple Endmember Spectral Mixture Models." *Remote Sensing of Environment*, Vol. 65, pp. 267−279.

CURRICULUM VITAE

Candidate's full name: Jianjun Wang

Universities Attended:

Peking University, Beijing, China, 1988-1992, B.Sc. in Geography

Publications:

Paper 1 (peer reviewed):

Wang, J.J., Y. Zhang, and C. Bussink (2013) "Remote Sensing of Opium Poppy Fields Using EO-1 Hyperion Hyperspectral Data: an Example in Afghanistan." *Proceedings of the 2013 Canadian Institute of Geomatics Annual Conference and the 2013 International Conference on Earth Observation for Global Changes (EOGC'2013)*, 5-7 June 2013, Toronto, Ontario, Canada.

Paper 2 (peer reviewed):

Wang, J.J., Y. Zhang, and C. Bussink (2013) "An unsupervised MTMF-based method for detecting opium poppy fields in Helmand, Afghanistan, from EO-1 Hyperion data." (submitted to *International Journal of Remote Sensing*)

Paper 3 (peer reviewed):

Wang, J.J., and Y. Zhang (2013) "An unsupervised approach to detect opium poppy fields in Bati Kot, Nangarhar, Afghanistan, using EO-1 Hyperion data." (to be submitted to *Remote Sensing (peer-reviewed Open Access journal)*)

Paper 4 (peer reviewed):

Wang, J.J., Y. Zhang, and C. Bussink (2013) "Can EO-1 ALI data detect opium poppy fields in Helmand, Afghanistan?" (to be submitted to *Remote Sensing (peer-reviewed Open Access journal)*)